PUB-5182
April 1988

Report on
Lawrence Berkeley Laboratory

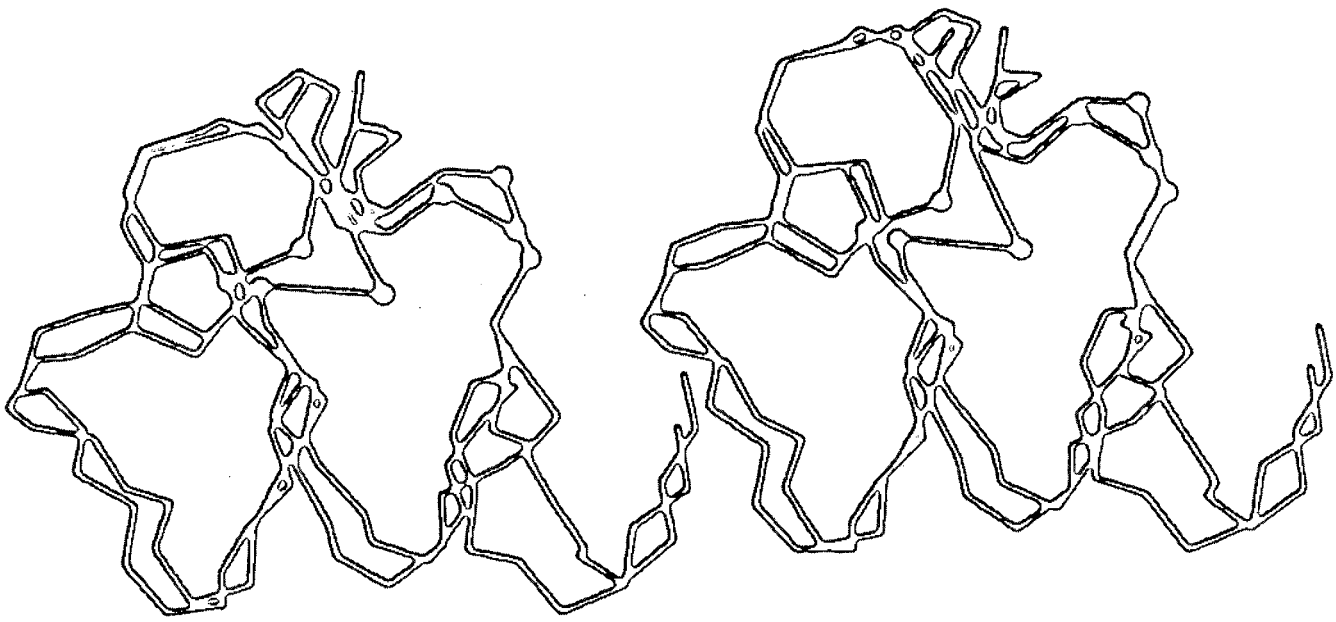

Program Development Fund
FY 1986

Prepared by
Office for Planning and Development

Lawrence Berkeley Laboratory
University of California
Berkeley, California 94720

Prepared for the U.S. Department of Energy under Contract No. DE-AC03-76SF00098

DISCLAIMER

Report on
Lawrence Berkeley Laboratory

Program Development Fund

FY 1986

Prepared by
Office for Planning and Development

Lawrence Berkeley Laboratory
University of California
Berkeley, California 94720

Prepared for the U.S. Department of Energy under Contract No. DE-AC03-76SF00098

Table of Contents

Introduction

Background

The Program Development Fund (PDF) was established at the Lawrence Berkeley Laboratory (LBL) in August 1984, following the issuance of Department of Energy Order 5000.1, Chg. 1, "Guidelines for Use of R&D Exploratory Funds," in December 1983. Funding for this program is allocated from the Laboratory's operating budget and is subject to approval by the Laboratory's Overhead Task Force, the Director, and the Department of Energy.

It is the objective of the fund to encourage innovative research to maintain the Laboratory's position at the forefront of science. Funds are to be used to explore new ideas and concepts that may potentially develop into new directions of research for the Laboratory and that are consistent with the major needs, overall goals, and mission of the Laboratory and the Department of Energy.

The types of projects eligible for support from PDF include:

- Work in forefront areas of science and technology for the primary purpose of enriching Laboratory research and development capabilities.
- Advanced study of new hypotheses, new experimental concepts, or innovative approaches to energy problems.
- Experiments directed toward "proof of principle" or early determination of the utility of a new concept.
- Conception, design analyses, and development of experimental devices, instruments, or components.
- Workshops and conferences that explore the present state of knowledge and the potential for significant advances in science or technology. (Funds for these activities were set aside and administered by the Deputy Director throughout the year.)

Process

In May 1985, the call for FY 1986 proposals for PDF was distributed to the Associate Directors. In response to this call, investigators submitted proposals to their cognizant Associate Director. The Associate Directors then reviewed the proposals and sent them on, with their comments, to the Director's Office. The proposals were reviewed by the Director's Review Committee, composed of the Director, the Deputy Director, and the Associate Director for Planning and Development. Projects were selected for funding, and most of the available funds were allocated. The remaining funds were reserved to fund worthy projects arising later in the fiscal year.

The requirements of DOE Order 5000.1, Chg. 1, were carefully considered during the selection process, to identify the extent to which proposals were consistent with the criteria. The ability to provide funds for exploratory R&D is vital to LBL's future growth and success and, as such, is given significant management attention.

Summary of Projects

In FY 1986, 78 proposals were submitted, requesting a total of $8.2 M. Of these, 28 projects were funded with a total allocation of $2.8 M. In some cases, approved projects were combinations or subsets of submitted proposals. Some approved projects received lower funding than that requested. Later in the fiscal year, the funding levels of all projects were reduced 4.3% across the board due to the Gramm-Rudman-Hollings sequestration. The projects funded in FY 1986 are listed in Table 1.

In the Project Reports section, accomplishments are summarized based on year-end reports submitted by the Principal Investigators. Several examples serve to indicate the importance and value of these projects to the Laboratory and the Department of Energy. Some of the projects explored new scientific theories. As an example,

Table 1. FY 1986 Program Development Fund Projects

Division	Investigator	Project	$K
Accelerator and Fusion Research Division			
	M. R. Howells	Ultra-High Resolution Grating Monochromators	116
	M. R. Howells	Contact X-Ray Microscopy Station	68
	K.-J. Kim	Novel Applications of Short-Period Undulators	77
Applied Science Division			
	T. Novakov	Fourier Transform Infrared Telescope	48
Biology and Medicine Division			
	J. C. Bartley	Center for Cellular and Molecular Cancer Biology	120
	P. H. Silverman	Hematozoa and Erythropoiesis	132
Center for Advanced Materials			
	M. Alper	Enzymatic Synthesis of Materials	77
	R. M. Cannon	Formation and Degradation of Protective Coatings	144
	J. W. Morris, Jr.	Theory of Phase Transformations	30
	M. B. Salmeron	Tunneling Microscopy of Catalysts	111
	D. S. Soane	Molecular Composites	20
Chemical Biodynamics Division			
	J. C. Bartholomew	Tissue-Specific Expression of Ri T-DNA Genes	35
	H. M. Frei	Conversion of Singlet Molecular-Oxygen	28
	J. E. Hearst	Photosynthetic Gene Expression	17
	D. Wemmer	NMR Studies of Biopolymers	35
Earth Sciences Division			
	O. Weres	Removal of Selenium from Groundwater	29
	P. A. Witherspoon	Downhole Shear and Compressional Wave Source	121
Engineering Division			
	B. W. Loo	New Compton Densitometer	76
Materials and Molecular Research Division			
	L. C. De Jonghe	Particulate Composite Structural Ceramics	92
	G. M. Rosenblatt	Raman Studies of Surface Processes	191
	P. N. Ross	Structure Determination at Metal/Solution Interface	68
	P. Y. Yu	Soft Phonon Modes and Solid-Solid Phase Transitions	28
Nuclear Science Division			
	W. M. Geist	Search for Quark-Gluon Plasma	123
	D. C. Hoffman	Large Einsteinium Activation Program	92
	L. S. Schroeder	Workshops and Planning	29
Physics Division			
	S. C. Loken	XXIII International Conference on High Energy Physics	21
	R. A. Muller	Automated Telescope Software and Hardware	191
	D. R. Nygren	Advanced Semiconductor Devices	246
	B. Sadoulet	Development of Gas-Scintillation Drift Chamber	66
	G. H. Trilling	Antiproton 30th Anniversary Celebration	17
Total			**2,448**

research on the development of theories to explain the behavior of materials was supported in the area of metal phase transformations. A theoretical model was developed and applied to the structure and ordering of liquid-solid transitions in aluminum-lithium alloys, which may be of significant importance for light alloy development in the aerospace industry. Experimental data showed good quantitative agreement with the models, which may be important for the design of high-temperature alloys needed for proposed ultra-high velocity supersonic aircraft.

Other projects initiated the development of prototype instrumentation. For example, a novel approach to ultra-high resolution microscopy was developed utilizing x rays, which cannot be focused with conventional lenses or mirrors. The technique developed was a contact x-ray microscopy station, which opens the door to further advances in microscopy far beyond the visible spectrum. Another example is the development of a new instrument, based on gamma-ray scattering, for measuring the density of living tissue. The Compton densitometer provides a noninvasive, portable, fast, accurate, and inexpensive method for measuring pulmonary edema. Radiation exposures with this instrument are a thousand times smaller than a typical chest x ray.

Other instrumentation-related research explored the possible applications of novel configurations of x-ray radiation-generating diagnostic instrumentation. Undulators and wigglers are magnetic insertion devices for electron synchrotrons that produce extremely bright, phased radiation that may have powerful diagnostic and imaging applications. The applications of short-period undulators were explored utilizing a "crossed undulators" configuration that can produce variably polarized x rays. This technique shows great promise for diagnosing the energy distribution of electrons in intense electron beams.

Some of the projects supported the exploration of new research programs that may have long-term national benefits. An example of this is the research project focusing on the development of new enzymatic techniques for the synthesis of novel polymeric materials that was initiated in FY 1986. The project initially demonstrated the modification of a natural enzyme to increase catalytic efficiency and yield of specific amino acid products. Production of amino acid oligomers, a precursor to the enzymatic synthesis of novel polymeric materials, has been achieved. This seed funding has resulted in a successful new LBL program in advanced materials research.

The development of coordinated research programs directed toward critical scientific problems that integrated diverse Laboratory expertise was also supported. The Center for Cellular and Molecular Cancer Biology was initiated to bring together cellular and molecular biologists to study the regulatory basis involved in the transformation of cells from normal to malignant conditions. Human mammary epithelial cells were used as the primary model system by a group of investigators. The researchers detected specific differences in surface chemistry in the cell membranes between transformed and normal cells. The approaches used in the Center are directly applicable to determining the stages in cell differentiation where transformation occurs. Research in the Center contributed to further biological research on the molecular basis of carcinogenesis and mutagenesis, which is becoming a more prominent research direction for the life sciences at LBL.

Project Reports

Accelerator and Fusion Research Division

Research on Ultra-High-Resolution Grating Monochromators

Principal Investigators: Malcolm R. Howells and Henning Hogrefe

Funding: $115,600

Project Description

An optimum configuration, with unrivaled energy resolution, for an ultra-high-resolution grating monochromator and its illumination system was developed using spherical diffraction gratings. Work involved analytical studies, including optical-path function expansion and computer modeling using the method of exact geometrical ray tracing.

Accomplishments

A spherical grating monochromator (SGM) has been designed that combines the advantages of designs providing high spectral resolution with those of designs offering good light-gathering power and a simple scan mechanism. The design is based on a principle originally proposed for application to space telescopes, where spatial and spectral resolution, as well as light-gathering power, are the principal concerns.

Spatial resolution is less critical for synchrotron radiation applications, but other constraints become more important. For example, a fixed exit direction is required, as is a scan mechanism compatible with ultra-high vacuum. In addition, the monochromator should be able to deal with relatively large sources, such as the one at Stanford Synchrotron Radiation Laboratory. Most of these demands can be met with the modified Rense-Violett system shown in Figure 1. This system consists of a toroidal condensing mirror M1, a spherical grating G, and entrance and exit slits S1 and S2, which are both movable along the beam.

To evaluate the optical performance of this monochromator design, a path-function analysis was carried out first, and then the performance was confirmed with a ray-tracing computer program. The path-function analysis produced theoretical estimates of the various aberrations that contribute to the overall energy resolution and showed that, within a range of wavelengths (depending on the optical parameters for the monochromator), the resolution is slit width limited for a 10-micrometer slit. Results from the ray-tracing program SHADOW confirmed this prediction, using a realistic Gaussian synchrotron source and assuming a random ray distribution. The slit-width-limited resolution is attainable with this monochromator design if other resolution-limiting factors (for example, optical-surface quality and geometrical stability) are held within tolerances believed to be reasonable and achievable.

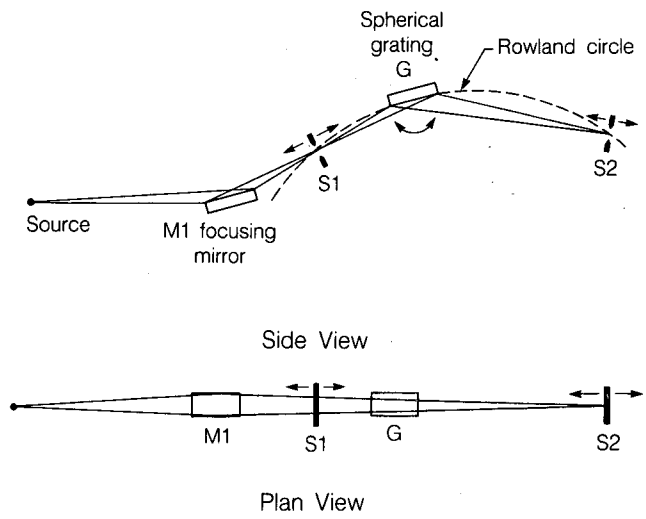

Fig. 1. Optical layout of high resolution spherical grating monochrometer.

Establishment of Contact X-Ray Microscopy Station and Application to the Study of Sickled Blood Cells

Principal Investigators: Malcolm R. Howells and Marcos F. Maestre

Funding: $68,100

Projection Description

A high-resolution contact x-ray microscopy station was established at the Center for X-Ray Optics and its capabilities were exploited to enhance studies of sickled blood cells.

Accomplishments

The basis of contact x-ray microscopy of biological samples is absorption by the carbon and nitrogen K edges, within the so-called water window between 23.6 and 44.8 Å. As shown in Figure 2, a sample is placed on a resist and then put into a sample chamber for exposure to x rays. The resist is usually polymethylmethacrylate (PMMA), which is spun onto silicon or Si_3N_4 wafers. Once the resist is exposed, it is developed in methyl isobutyl ketone (MIBK) or a solution of MIBK and isopropyl alcohol. The result is a relief map that may be viewed by an electron microscope (see Figure 3). In addition to being uniquely applicable to studies of biological samples in their "wet" or "living" state, contact microscopy might also serve as the basis for soft-x-ray microanalysis (i.e., elemental mapping), stereoscopic imaging, and optical-element replication.

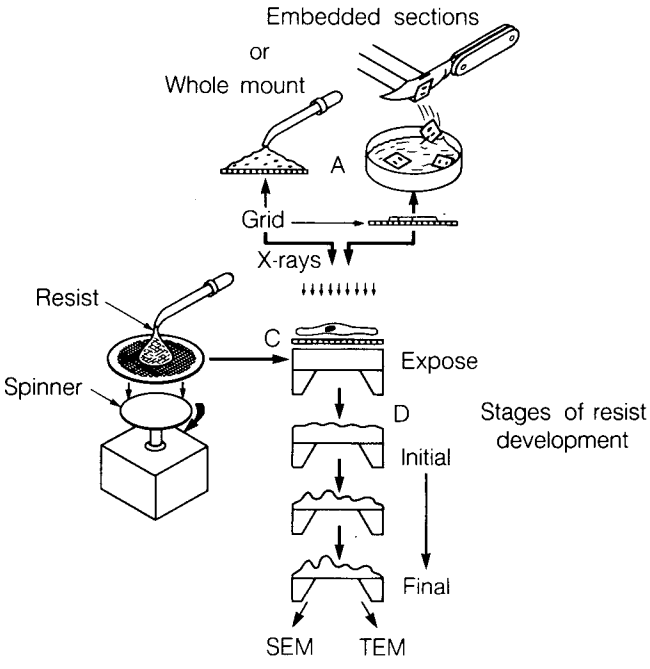

Fig. 2. Procedure for doing soft-x-ray contact microscopy or lithography.

As shown in Figure 3, fabrication of a microscopy station (only a handful presently exist worldwide) has been completed, and its capabilities have begun to be exploited. It was determined that a commercial electron-beam evaporator with a well-cooled target could be used to generate soft monochromatic x rays in high vacuum ($\sim 10^{-6}$ to 10^{-7} Torr). The target material now being used is vanadium, chosen for use of its L emission lines, though other materials may easily be used. A typical exposure now requires 8 to 12 hours.

The continuing aim is to use the microscopy station to image sickled and normal red blood cells and to observe the effect of oxygen tension on hemoglobin S and A. Preliminary x-ray micrographs of red blood cells provided by Dr. Stephen Embury, a hematologist at U.C. San Francisco, have been obtained. Work is continuing to improve the quality of these images, as are efforts to understand the micropolymerization processes that occur with the hemoglobin S.

Research into Novel Applications of Short-Period Undulators

Principal Investigator: Kwang-Je Kim

Funding: $77,000

Project Description

A rigorous formulation of the brightness concept in terms of the Wigner distribution, including polarization and encompassing applications to radiation propagation and imaging was developed. Transverse radiation profiles, which will ultimately have implications for phase-sensitive techniques such as microholography, were studied. Novel sources of radiation that provide a variable polarization capability, such as crossed undulators, were also proposed.

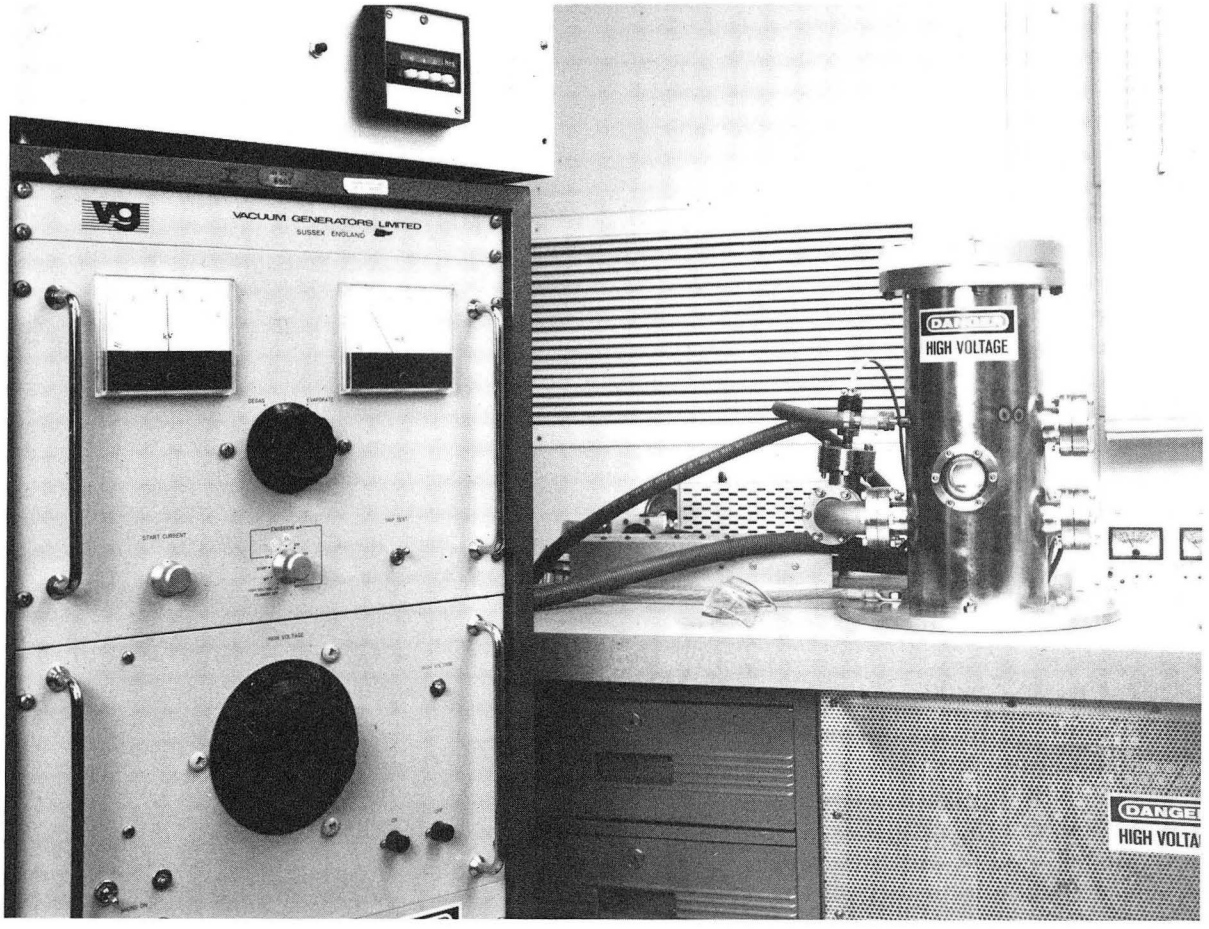

Fig. 3. The soft-x-ray contact microscopy station in operation.

Accomplishments

A broader understanding of undulator capabilities has been developed by addressing the phase-space characterization of undulator radiation and by proposing a novel scheme for using a pair of wigglers as a diagnostic device for measuring the energy distribution of a stored electron beam.

Phase-Space Characterization of Undulator Radiation. To describe how undulator radiation propagates through optical elements such as lenses or free space and how images and interference patterns are formed, it is necessary to understand the flux distribution in angle-position phase space. The flux density in phase space is known as the brightness, which, being invariant under optical transformations, is a true characterization of the source strength. Until now, such a formulation has not been available for synchrotron radiation, and the discussion of the radiation characteristics has been limited to the angular distributions.

A phase-space formulation of synchrotron radiation optics based on the Wigner distribution function has now been developed. This provides a rigorous meaning for the concept of brightness, thus clarifying the relationship between the radiation phase space and the electron phase space. Based on this work, it will be possible in the future to develop a more complete "ray-tracing" program for synchrotron radiation that includes effects due to diffraction.

An Interference Wiggler for Precise Electron-Beam Energy Diagnostics. A pair of crossed undulators can be used as a source of variably polarized radiation. The first steps have now been taken toward developing another device, called an interference wiggler, which is a pair of parallel wigglers that can be used for precise diagnostics of electron-beam energy. The interference wiggler is similar in structure to a transverse optical klystron, except that the multiperiod undulators are replaced by simple,

three-pole wigglers. The radiation spectrum from the device exhibits rapid modulation, the details of which contain information on the energy distribution of the electrons. In the future, interference-wiggler/monochromator systems for application to the Advanced Light Source and other electron machines, such as the Continuous Electron Beam Accelerator Facility, will be designed.

Publications

G.D. Guttmann and M.R. Howells, "Soft X-Ray Contact Microscopy," presented at the American Association of Physicists in Medicine Annual Meeting, Lexington, KY, August 1986; published in *Med. Phys. 13* (4), 603 (1986).

H. Hogrefe, M.R. Howells, and E. Hoyer, "Application of Spherical Gratings in Synchrotron Radiation Spectroscopy," *Proc. SPIE 733*, to be published.

K.-J. Kim, "Brightness, Coherence and Propagation Characteristics of Synchrotron Radiation," *Nucl. Instrum. Methods A246* , 71 (1986).

K.-J. Kim and N. King, "Photon Performance of a High Brightness, Soft X-ray and VUV Synchrotron Radiation Facility," LBL PUB-487 (1985).

K.-J. Kim and C. Pellegrini, "High-Gain Free Electron Lasers as Generators of Short Wavelength Coherent Radiation," *AIP Conf. Proc. 147*, 17 (1986).

K.-J. Kim, "Brightness and Coherence of Synchrotron Radiation and High-Gain Free Electron Lasers," presented at the VII National Conf. on Synchrotron Radiation (SR-86), Novosibirsk, USSR, June 1986, LBL-22317 (1986); to be published in *Nucl. Instrum. Methods.*

K.-J. Kim, "Three-Dimensional Analysis of Coherent Amplification and Self-Amplified Spontaneous Emission in Free Electron Lasers," *Phys. Rev. Lett. 157*, 1871 (1986).

Applied Science Division

Fourier Transform Infrared Telescope: High-Resolution Studies of the Atmosphere

Principal Investigator: Tihomir Novakov

Funding: $48,400 (second year of funding)

Project Description

A Fourier Transform Infrared (FTIR) telescope was used to identify and quantitate radiatively important trace gases in the ambient atmospheric column.

Accomplishments

Using the sun as a broadband infrared source, the absorption spectrum of the total atmospheric column may be recorded with the FTIR telescope, on different days, both under clean and polluted conditions. Absorption lines due to many gaseous species of anthropogenic origin are clearly identifiable. Lines due to carbon dioxide and methane can be clearly resolved and fit to a Lorentzian line shape, and their total integrated absorbance determined. This integrated absorbance is directly proportional to the total atmospheric column burden of the gaseous species, with contributions to the line shape from molecules at various altitudes in the atmosphere dependent on the temperature and pressure at that altitude. Temperature and pressure profiles in the atmosphere do not vary appreciably from day to day, nor do the concentrations of methane and carbon dioxide measured above the boundary layer. Thus, the total column spectral line absorbance for these species is not expected to show a natural variability of more than a few percent on a day-to-day basis. Increases in absorbance above this background are then attributed to increases in the carbon dioxide and methane concentrations at low altitudes in the urban boundary layer overlying the San Francisco Bay Area. By taking a reasonable range of values for the depth of this layer, the increase in concentration within the layer that would be required to produce the observed increase in total column absorbance can be calculated. These pollutants, as well as many other gaseous species of anthropogenic origin, are active infrared absorbers, and increases in their concentration in urban areas could lead to increased thermal trapping and the intensification of the urban heat island, i.e., localized climatic change. Observations and understanding of these phenomena on a local scale will greatly assist model calculations of the global "greenhouse" effect.

This approach is unique in that a ground-based measurement (i.e., infrared spectrometry) can lead to a calculation of a pollutant increase within the entire depth of the urban atmospheric boundary layer. Ground-level analyses for trace constituents of the atmosphere can yield these results for the composition of the surface air but give no information as to the depth of the atmosphere into which the pollutants are mixed. By extending the scanning to cover the entire hemispheric sky field of view, tomographic reconstruction can conceivably be used to map the three-dimensional distribution of these compounds over an urban or other source area.

This project was completed during FY 1986. The observed spectra show large changes in integrated absorbance for a series of 35 noon measurements taken over a nine-month period, as shown in Figure 1. The smallest of these measurements are

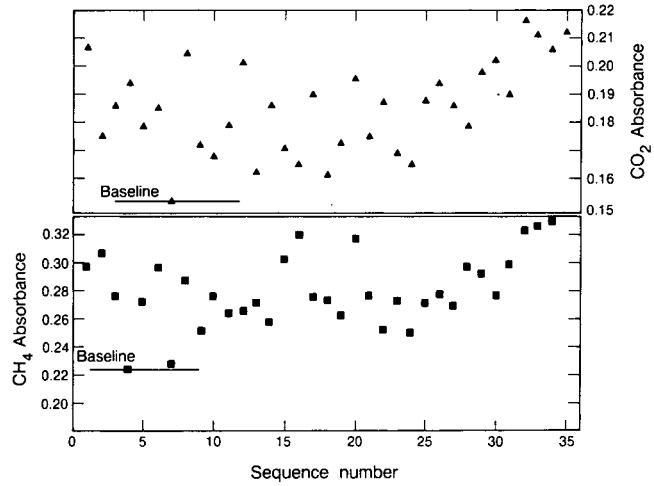

Fig. 1. Time series of methane and carbon dioxide whole column absorbance.

designated as the "clean-air background" atmospheric column absorbance. The large measured increases in absorbance above this background imply large carbon dioxide and methane increases in the urban boundary layer on polluted days.

Publications

K.R. Gurney, A.D.A. Hansen, and H. Rosen, "Methane and Carbon Dioxide Increases in the Urban Boundary Layer: Inferences from Whole-Column Infrared Absorbance Measurements," LBL-22289, to be submitted to Geophysical Research Letters (1986).

Biology and Medicine Division

Center for Cellular and Molecular Cancer Biology

Principal Investigators: John C. Bartley, Priscilla K. Cooper, Michael S. Esposito, Regine Goth-Goldstein, Junko Hosoda, S. Anthony Leadon, Gordon Parry, and Martha R. Stampfer

Funding: $119,700

Project Description

A coordinated, interdisciplinary approach for the study of carcinogenesis and mutagenesis at LBL was initiated. The immediate goal is to foster a multi-investigator collaboration to address fundamental problems in cancer biology at the biochemical, molecular, and cellular levels. In the long term, it is anticipated that the collaborations and information generated will be the first step in establishing a broad base of stable support for the carcinogenesis/mutagenesis program at LBL.

Accomplishments

Five specific projects were targeted for support during the first year of this initiative and were designed to bring an integrated, multi-investigator approach to the study of carcinogenesis/ mutagenesis at LBL. The preliminary results indicate that the following three projects may evolve into mature initiatives in cancer research:

- Basis for Resistance to Alkylating Carcinogens (Goth-Goldstein, Leadon, Cooper)
- Oxidative Damage in DNA of Human Mammary Epithelial Cells Following Low-Level Irradiation (Leadon, Stampfer, Yang, Bartley)
- Analysis of Cell-Surface Proteins in Normal and Transformed Human Mammary Epithelial Cells (Parry, Bartley, Stampfer)

Basis for Resistance to Alkylating Carcinogens. CHO (Chinese hamster ovary) cells and mer HeLa (human) cells are deficient in the removal of the lethal and mutagenic DNA adduct formed at the O^6 position of guanine by alkylating carcinogens. It has recently been found that both CHO and HeLa cells surviving treatment with a highly toxic dose of methylating agents have a permanently increased resistance to these agents. Overall repair capacity does not appear to be altered in the resistant cells, and adducts are formed at the same frequency as in the sensitive population. This collaborative project seeks to identify the molecular basis for the increased resistance. In particular, the hypothesis that the resistant cells are better able to repair damage in critical regions of the genome will be tested in two ways: (1) the possibility that actively transcribing genes are preferentially repaired will be tested using monoclonal antibodies to select repaired DNA followed by hybridization using probes for specific DNA sequences, and (2) the possibility that DNA undergoing replication is preferentially repaired will be tested by adapting a technique with *E. coli* for separation of replicating from nonreplicating regions of the genome by two-dimensional agarose-gel electrophoresis of restricted pulse-labeled DNA. With respect to the second approach, preliminary studies indicate that the technique for analyzing repair in replication forks separate from nonreplicating regions of the genome can be adapted to isolation of mammalian DNA, even though this DNA is in a more complex configuration.

This technique is currently being applied to resistant and sensitive cell lines exposed to various methylating agents. Understanding the basis for induction of resistance in mammalian cells could provide profound insights into the mechanisms for DNA repair and the basis for familial susceptibility to cancer.

Oxidative Damage in DNA of Human Mammary Epithelial Cells Following Low-Level Irradiation.

The goal of this initiative is to determine the effect of repeated exposures to very low level (minimal toxicity) irradiation (x or gamma rays) on human mammary epithelial cells in culture. Low-level irradiation has been selected in an attempt to mimic clinical and accidental exposures *in vivo*. Such a study is possible for the first time because: (1) a unique culture system for growing normal human mammary epithelial cells (HMEC) has been developed; (2) collaborative studies have firmly established the cell survival curves after irradiation of these cells; and (3) there

is a unique antibody for thymine glycol that is of proven value in quantifying the oxidative damage to DNA following irradiation.

Human mammary epithelial cells (HMEC) have been shown to metabolize the carcinogen benzo(a)pyrene (B(a)P) efficiently; B(a)P can be converted to a very reactive electrophile that forms covalent DNA adducts and other metabolites. These metabolites can give rise to free-radical intermediates and reactive reduced-oxygen species as a result of autoxidative processes and oxygen-reduction cycles. These cycles are coupled with molecular oxygen to form reactive oxygen species such as superoxide anions and hydrogen peroxide. HMEC cultures were exposed to various doses of the carcinogen for four hours, and thymine glycols and covalent adducts were produced in the DNA in a dose-dependent manner (Figure 1). At a BaP concentration of 1 μg/ml, the frequency of thymine glycol formation and covalent B(a)P adducts per 10^6 bases was similar. Since thymine

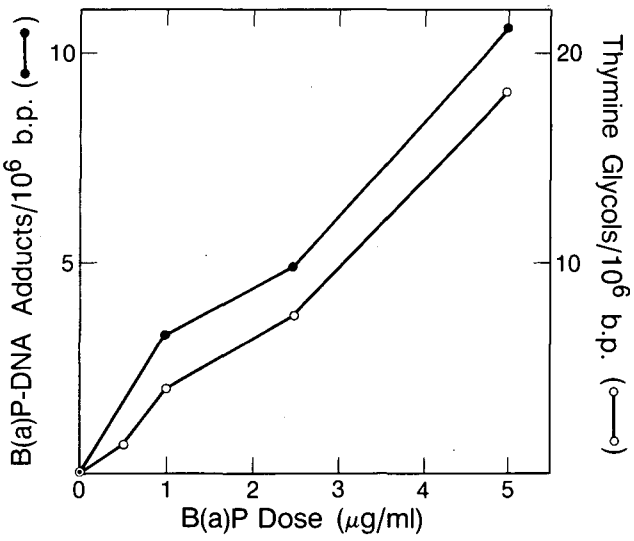

Fig. 1. Production of B(a)P-DNA adducts and thymine glycols in DNA from B(a)P treated HMEC cultures. Cells were exposed to various concentrations of [^{3}H]B(a)P for 4 h. Total B(a) P adduct frequencies were derived from the ^{3}H radioactivity in the purified DNA and from the specific activity of the [^{3}H]B(a)P preparation. Thymine glycol frequencies were determined in a competitive ELISA by reacting antibody (1:1000 dilution) with 50 ng OsO_4-oxidized DNA (0.04% thymine glycols).

glycols are only one type of DNA lesion produced by active oxygen, the damage produced by the indirect action represents a large fraction of the total damage induced by metabolism of B(a)P in HMEC.

Because hydroxyl radicals are responsible for the majority of the biological effects of ionizing radiation on DNA, a comparison was made between their formation in HMEC following exposure to either B(a)P or gamma rays. At equitoxic doses of both agents (30–40% survival), the efficiency of thymine glycol formation was approximately 35-fold greater in HMEC cultures exposed to B(a)P than to gamma rays. Therefore, even though the damage produced by indirect action during the metabolism of B(a)P represents a large fraction of the total damage produced, not all of this damage appears to play a role in cell killing. Its overall importance, however, may be related to the carcinogenesis potential of B(a)P.

Repair of DNA damage was also investigated in the HMEC. Thymine glycols produced by B(a)P metabolism were removed from the DNA of HMEC with about the same efficiency as was found for thymine glycols produced by ionizing radiation, even though there was a significantly greater initial frequency of this damage following exposure to the carcinogen. By 45 minutes post treatment, approximately half of the initial thymine glycols had been removed. During this same repair time, little or no loss of B(a)P adducts from the DNA was observed.

Catalase and superoxide dismutase (SOD) break down hydrogen peroxide and superoxide anions, respectively. Currently, HMEC are being incubated with B(a)P in the presence of one or both of these enzymes to test the effect on survival or extent of DNA damage. Initial results indicate that SOD, but not catalase, protects the cells against the toxic effects of B(a)P. This effect appears to be due to a decrease in the amount of oxidative damage (Table 1).

Analysis of Cell-Surface Proteins in Normal and Transformed Human Mammary Epithelial Cells. The expression of surface antigens is being determined by the use of monoclonal antibodies developed in response to the human milk fat globule membrane, which is derived from the apical plasma membrane of mammary epithelial cells. Using antibodies in an indirect immuno-fluorescence assay, differences among the surface components of normal, tumor-derived, and

Table 1. Effect of superoxide dismutase and catalase on production of thymine glycols, production of B(A)P-DNA adducts, and survival in human mammary epithelial cells exposed to benzo(a)pyrene.

Treatment	Thymine Glycols per 10^6 bp	B(a)P Adducts per 10^6 bp	Percent Survival
None	—	—	100
2.5 μg B(a)P	9.0	8.0	29
2.5 μg B(a)P + 10 μg SOD	9.0	9.0	17
2.5 μg B(a)P + 50 μg SOD	7.0	7.0	47
2.5 μg B(a)P + 100 μg SOD	1.8	6.0	75
2.5 μg B(a)P + 250 μg SOD	N.D.[a]	N.D.	96
2.5 μg B(a)P + 100 μg catalase	8.0	N.D.	17
2.5 μg B(a)P + 100 μg catalase + 100 μg SOD	2.0	N.D.	58

[a] N.D., not determined

chemically transformed HMEC cultures can be demonstrated. The protein and sugar content of these cell-surface molecules will be analyzed using Western blots and routine biochemical techniques. Since the cell surface determines many aspects of tumor-cell behavior (invasiveness, cell-cell recognition, response to immunological and therapeutic agents), this study may elucidate crucial determinants of malignancy.

After screening six antibodies for their ability to bind the cell surface of HMEC, three were selected for further study on the basis of the immunocytochemistry. The results indicate that antibody P2C1 may be useful in distinguishing between normal cells and those of the transformed lines A1 and B5, but the expression is not modulated by the different media (MCDB 170 and MM). In contrast, expression by normal cells of the surface molecules with affinity for antibodies P2A1 and P3B1 is modulated by the growth medium. However, one of these, P2A1, reacts with the surface component on transformed cells, whereas the component reacting with P3B1 on these cells does not. The differential staining and differences in response to growth medium may help to identify stages of differentiation in normal cells and distinguish between normal and transformed cells in mixed cultures. In those cultures showing less than 10% positive cells, treatment of the cells with an enzyme removing a specific carbohydrate component may help to amplify differences between normal and transformed cells.

The molecules involved in the expression of glycolipids and glycoproteins on the surface of these cells are being actively studied to provide a rational basis for identification of the stages of differentiated functions in HMEC and to provide a partial basis for detection of HMEC transformed in culture.

Hematozoa and Erythropoiesis: Effects of Malaria Infection

Principal Investigators: Paul H. Silverman and Lynn J. Mahlmann

Funding: $132,400 (second year of funding)

Project Description

Anemia and immunosuppression are complications associated with malaria infection. The biological mechanisms leading to these disease characteristics are only partly understood. Numerous studies have demonstrated that red-cell destruction by the plasmodial parasite is inadequate to account for the severity and extent of anemia caused by malaria. It has been suggested that anemia and immunosuppression might be due to the impairment of progenitor hemopoietic cells or an imbalance in the competition between red cell and immune-cell lineages derived from a common pluripotent stem cell (CFU-s) (Figure 2).

Accomplishments

During the first year of the project, it was demonstrated that infection with three species of murine malaria resulted in substantial quantities of erythropoietin (EP) being produced and made available in the circulating plasma. Erythropoietin is the hormone responsible for regulating red-cell production by committed erythron progenitors. It has also been found that colony stimulating factors (CSF), which regulate the proliferation and differentiation of granulocytic and monocytic cells, are stimulated in increased quantities during infection with malaria. These findings suggest that the dyserythropoiesis observed in malaria-infected hosts might be

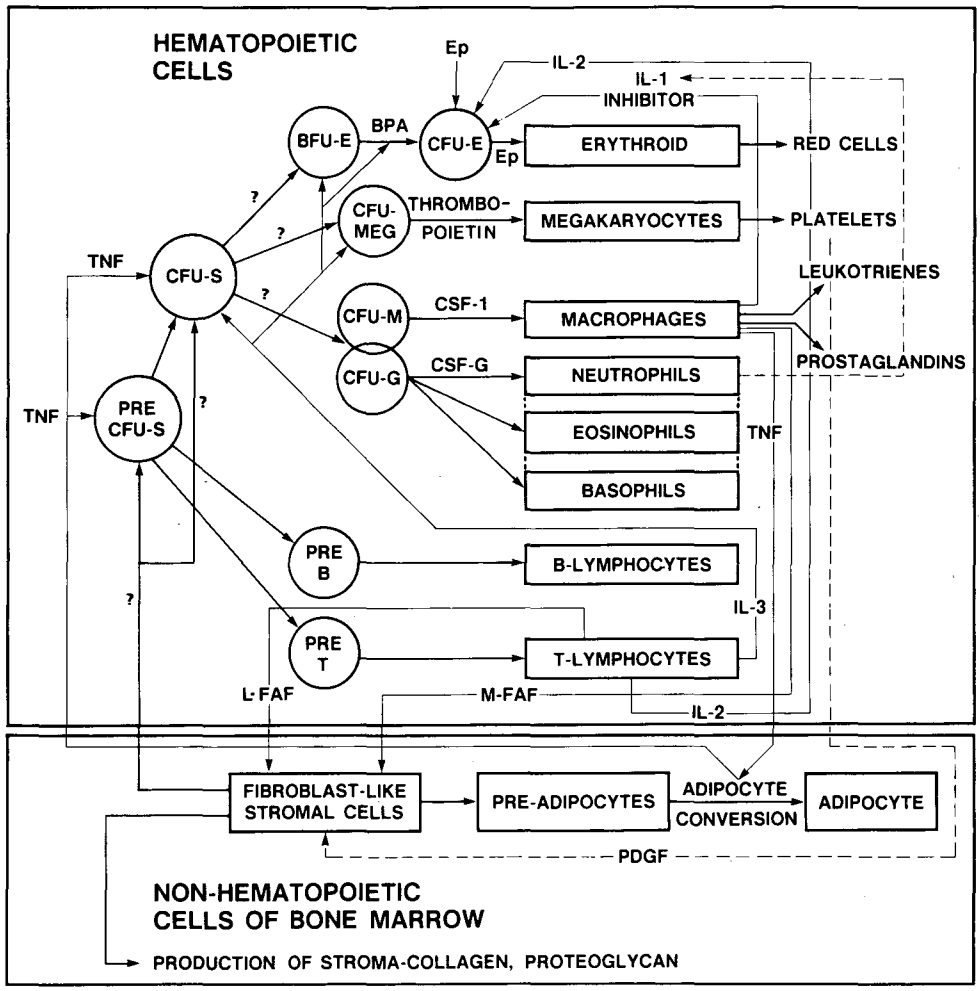

Fig. 2. Complex interrelationships between various cells of the hematopoietic system and the various cytokines produced. TNF = tumor necrosis factor; FAF = fibroblast activating factor; BPA = burst promoting activity; CSF = colony stimulating factor; PDGF = platelet derived growth factor.

caused by events inhibiting progenitor differentiation and amplification or by the lack of progenitor-cell production by stem cells. The results indicate that both situations occur during malaria infection.

Infection with two lethal strains of murine malaria, *Plasmodium berghei* and *P. vinckei*, results in significant depletion of pluripotent stem cells in the bone marrow. Similar depletion occurs with a nonlethal strain of malaria, *P. chabaudi adami*. Maximum depletion of bone-marrow stem cells coincides with the maximum parasitemia. As the self-limiting infection with *P. chabaudi adami* runs its course, stem-cell levels and the total cellularity of the bone marrow return to normal.

Although stem cells and total cellularity returned to normal or above normal levels when red-cell parasitemia became negative, evidence remains that a substantial migration of stem cells occurs in malaria-infected mice. The increased number of stem cells observed in the spleen and circulating in the blood may account for the bone-marrow depletion. However, whether splenic and circulating stem cells are functionally equivalent to bone-marrow stem cells remains to be determined. Similar observations were made in mice infected with lethal infections of *P. berghei* and *P. vinckei*. The observations made with *P. chabaudi adami* infection enabled more extensive evaluations to be made of stem-cell kinetics. Determination of the rate of stem-cell proliferation by assessing the killing effects of hydroxyurea indicated that DNA synthesis in stem cells in bone marrow or spleen was comparable to that which occurs in normal mice. Similar observations are needed of stem cells recovered during active infections before the impact on DNA synthesis can be fully evaluated.

It is proposed that stem-cell depletion in bone marrow is induced by a diffusable substance. Several candidate substances have been identified, including tumor necrosis factor (TNF). TNF (or cachectin) is produced by macrophages and/or monocytes during the processing of malaria antigen. It has been reported that TNF inhibits adipocyte gene expression. Adipocytes are a major cellular component of the adherent stromal bone marrow and provide an essential environment for renewal and differentiation of the nonadherent hemopoietic stem cells. The inhibitory action of malaria-induced TNF might account for both the drop in total cellularity and the depletion of marrow hemopoietic stem cells. The effects of recombinant human TNF on stem cells in a murine model are reported here for the first time.

Because of the short half life *in vivo* of TNF, miniosmotic pumps containing rHuTNF in RPMI 1640 tissue-culture medium were implanted subcutaneously into female Balb/c mice. At an infusion rate of 1 μl/hr, the estimated plasma concentration of TNF was 13,200 units. Control mice were infused with RPMI 1640. After six days of infusion, the total CFU-s content of the blood, bone marrow, and spleen was determined using the spleen colony assay.

In many respects, after six days of infusion, the TNF-induced cellular changes in mice are very similar to those observed in malaria-infected animals. The total number of bone-marrow nucleated cells is decreased, a significant decrease in the number of bone marrow stem cells occurs, stem-cell levels in the spleen are greatly increased, and evidence of stem-cell migration is apparent by their presence in large numbers in the circulating blood (Table 2). Much more needs to be done to determine the specific cellular elements affected by rHuTNF in the murine model and also to determine how this compares with murine TNF.

The relevance of these observations to the production of TNF during malaria infection was tested by injecting monoclonal antibody prepared against rHuTNF into mice before infection with *P. vinckei* or *P. berghei*. Booster doses of 10 μg of the monoclonal antibody (Anti-TNF) were given every 72 hours until the mice were tested for CFU-s content. It was anticipated that the antibody might have a sparing effect on the deleterious effect of the malaria infection. The results suggest that some sparing effect on the bone-marrow stem-cell population of mice infected with *P. vinckei* occurred (Table 3). Although early observations indicated more dramatic protection effects, replicate experiments resulted in the data summarized in Table 2. It is highly probable that antigenic differences occur between human and murine TNF and might account for the lack of activity with the monoclonal antibody.

In addition to the potential role of TNF/cachectin in the pathogenicity of malaria, other work (reported by J.C. Schooley) has identified interleukins as contributors to the regulation of hemopoietic activity. The insights gained by

Table 2. Effect of infused rHuTNF[a] on CFU-s content in marrow, spleen and blood in Balb/c Mice.[b]

	N	cells $\times 10^{-6}$/organ nucleated cells	CFU-s/10^6	CFU-s/organ
Marrow				
rHuTNF	7	11.0 ± 0.41	190 ± 14[c]	2100 ± 130
RPMI-1640	7	13.6 ± 0.95	280 ± 23	3800 ± 160
Untreated	16	13.7 ± 0.50	280 ± 7.0	3900 ± 90
Spleen				
rHuTNF	7	130 ± 20	170 ± 14	27000 ± 2700
RPMI-1640	6	170 ± 3.5	20 ± 1.1	3500 ± 200
Untreated	6	134 ± 3.4	15 ± 0.84	2000 ± 100
		nucleated cells $\times 10^{-6}$/ml	CFU-s/10^7 cells	CFU-s/ml
Whole Blood				
rHuTNF	7	22 ± 5.1	240 ± 60[d]	520 ± 53
RPMI-1640	6	9.7 ± 1.4	11 ± 2.6	11 ± 1.9
Untreated	10	8.5 ± 0.71	4.2 ± 1.5	3.4 ± 1.3

[a] Supplied by Genentech.

[b] All values are expressed as the mean ± S.E.M. Untreated mice did not have subcutaneous implants of mini-osmotic pumps.

[c] $P < 0.01$.

[d] $P < 0.001$.

Table 3. Effect of anti-TNF monoclonal antibody[a] on bone marrow CFU-s in Balb/c mice infected with murine malaria[b]

	% pRBC[c]	CFU-s/10^6 BMC	CFU-s/femur	cells $\times 10^{-6}$/femur	
Control	0	290 ± 7.0	3900 ± 86	14 ± 0.50	16
Anti-TNF	0	290 ± 16	3500 ± 270	13 ± 0.39	4
		Plasmodium vinckei vinckei (Day 8)			
Infected	74 ± 3.9	280 ± 10.0	2400 ± 100	8.2 ± 0.49	8
+ Normal sera	76 ± 15	300 ± 18	2500 ± 140	8.4 ± 0.36	4
+ Anti-TNF	70 ± 7.8	360 ± 12	1300 ± 130	8.9 ± 0.79	7
		Plasmodium berghei (Day 10)			
Infected	50 ± 6.8	190 ± 12	1300 ± 90	6.4 ± 0.35	8
+ Normal sera	56 ± 11	280 ± 25	1760 ± 160	6.3 ± 0.19	3
+ Anti-TNF	61 ± 2.3	150 ± 15	1300 ± 150	7.4 ± 0.60	8

[a] Supplied by Chiron.

[b] All values are expressed as the mean ± S.E.M.

[c] pRBC = parasitized red blood cells.

analysis of this model system will have application to a basic understanding of hemopoiesis and might lead to manipulation of differentiation and proliferation of various cell lineages.

Publications

S.A. Leadon, "Production of Thymine Glycols in DNA by Radiation and Chemical Carcinogens as Detected by a Monoclonal Antibody," *British J. Cancer*, in press (1987).

G. Parry, M.R. Stampfer, and J.C.Bartley, "Expression of Multiple Epitopes on High Molecular Weight Glycoproteins (PAS-O-like Molecules) on Human Mammary Carcinoma Cells (734B) and Milk Fat Globule Membranes," presented at Second International Workshop on Monoclonal Antibodies, San Francisco, CA (1986).

P.H. Silverman, J.C. Schooley, and L.J. Mahlmann, "Erythropoietin and Bone Marrow Stem Cell Responses to Murine Malaria," 60th Annual Meeting American Society of Parasitologist, abst. #150, August 4–8, 1985, Athens, GA (1985).

P.H. Silverman, J.C. Schooley, and L.J. Mahlmann, "Murine Malaria Decreases Hemopoietic Stem Cells," *Blood 69*, No. 2, 408 (1987).

P.H. Silverman, J.C. Schooley, L.J. Mahlmann, and K.L. Smith, "Mechanisms of Hemopoietic Suppression by Murine Malaria," 35th Annual Meeting of the American Society of Tropical Medicine and Hygiene, abst. #121, December 7–11, 1986, Denver, CO (1986).

M.R. Stampfer, and J.C. Bartley, "Growth and Transformation of Human Mammary Epithelial Cells in Culture," in *Cellular and Molecular Biology of Experimental Mammary Cancer*, D. Medina, W. Kidwell, G. Heppner and E. Anderson, eds., Plenum Press, in press (1987).

Center for Advanced Materials

Enzymatic Synthesis of Materials

Principal Investigators: Mark Alper, Harvey W. Blanch, Jack F. Kirsch, and Peter G. Schultz

Funding: $77,300

Project Description

Living organisms, through the action of their enzymes, produce an extraordinary array of substances with widely differing structures and functions. Many of these substances have materials properties that make them suitable for nonbiological applications. This project is designed to examine enzymatically produced molecules and determine whether the specific and rational modification of the enzymes involved can lead to the synthesis of new materials of even greater usefulness.

The project has two components at this time:

1. Design and synthesis of modified enzymes that can catalyze new reactions in materials synthesis. These enzymes will be modified by substituting new natural or synthetic amino acids in the enzyme's protein chain.
2. Design of reactor conditions to use these enzymes in materials synthesis.

Both are being applied to model systems and also to enzymes that will actually be used to synthesize new materials.

Accomplishments

Work on enzyme modification using natural amino acids focused first on the demonstration that substrate specificity and catalytic activity could be altered through site-directed mutagenesis. Both goals have been achieved in the model system, aspartate aminotransferase (AATase).

First, arginine 292 has been replaced by an aspartate residue. The mutant enzyme, R292D, shows an increased catalytic efficiency toward the amino acid L-arginine over that of wild type enzyme, whereas the activity toward the natural substrate, L-aspartate, is reduced by over five orders of magnitude (Table 1). Thus, the mutant enzyme provides the first example of an inversion of substrate charge specificity by site-directed mutagenesis.

In addition, replacement of lysine 258 by alanine has been shown to result in a change in the reaction catalyzed. Natural AATase interconverts aspartate and oxaloacetate. The modified enzyme interconverts oxaloacetate and alanine and CO_2.

Materials synthesis will focus first on the enzyme lysozyme. Work is therefore proceeding on cloning and achieving expression of its gene. A clone of the hen egg-white lysozyme (HEWL) gene has been obtained. In collaboration with scientists at Chiron Corporation, it was inserted into yeast and engineered to facilitate secretion of the product. Yeast spheroplasts were transformed; levels of expression are under current investigation.

In parallel studies, a gene-fusion approach using the bacterial beta-galactosidase gene has been undertaken to obtain expression of the lysozyme gene in *E. coli*. If successful expression is obtained, the beta-galactosidase-HEWL linkage will be cleaved with a specific protease, separating the two proteins.

Work is also progressing on the system that will incorporate synthetic amino acids into enzymes (Figure 1). While awaiting availability of the lysozyme clone, the work here is focused on developing the DNA-dependent *in vitro* protein-synthesizing system using the model system, beta-lactamase. The most efficient such system

Table 1. AATase substrate specificity.

	k_{cat}/K_M $(M^{-1}s^{-1})$		
Substrate	Wild Type	R292D	Selectivity Ratio[a]
L-Arginine	2.8×10^{-2}	4.0×10^{-1}	14.1
L-Aspartate	1.9×10^{-4}	7.0×10^{-2}	3.8×10^{-6}

[a] k_{cat}/K_M: R292D/wild type.

reported has now been developed. Yields currently are in the range of 30–50 μg active beta-lactamase using both mutant (containing an amber nonsense codon at serine 70 position) and native leaderless genes. Enzyme synthesized *in vitro* has been shown to have activity similar to that of an enzyme purified from *E. coli*. The gene containing the amber nonsense codon affords no active enzyme when expressed either *in vitro* or *in vivo*. Current work is focused on a two-step purification of *in vitro* synthesized enzyme, which has produced encouraging preliminary results.

Work on the second component of the project, the study of the activity of lysozyme under materials-synthesis conditions, has also proceeded. The presence of water in the reaction mix would promote the enzymatic degradation of polymer rather than synthesis; thus alternative solvents must be found. Organics would solve this problem so long as lysozyme remains active in them. The new solvent must also solubilize the substrates. Experimental results show that lysozyme is active in 20% v/v solutions of two organic solvents, N,N-dimethylacetamide (DMA) and 1-methyl-2-pyrrolidinone (MP).

Production of N-acetylglucosamine (NAG) oligomers for use as substrates and technique development has also been achieved and separation performed by HPLC. High sensitivity is achieved by detection at 190 nm, allowing measurements of concentrations in the parts-per-million range.

Formation and Degradation of Protective Coatings

Principal Investigators: Rowland M. Cannon and Robert M. Fisher

Funding: $144,000

Project Description

The recently attained and still-developing basic understanding of oxide-formation mechanisms,

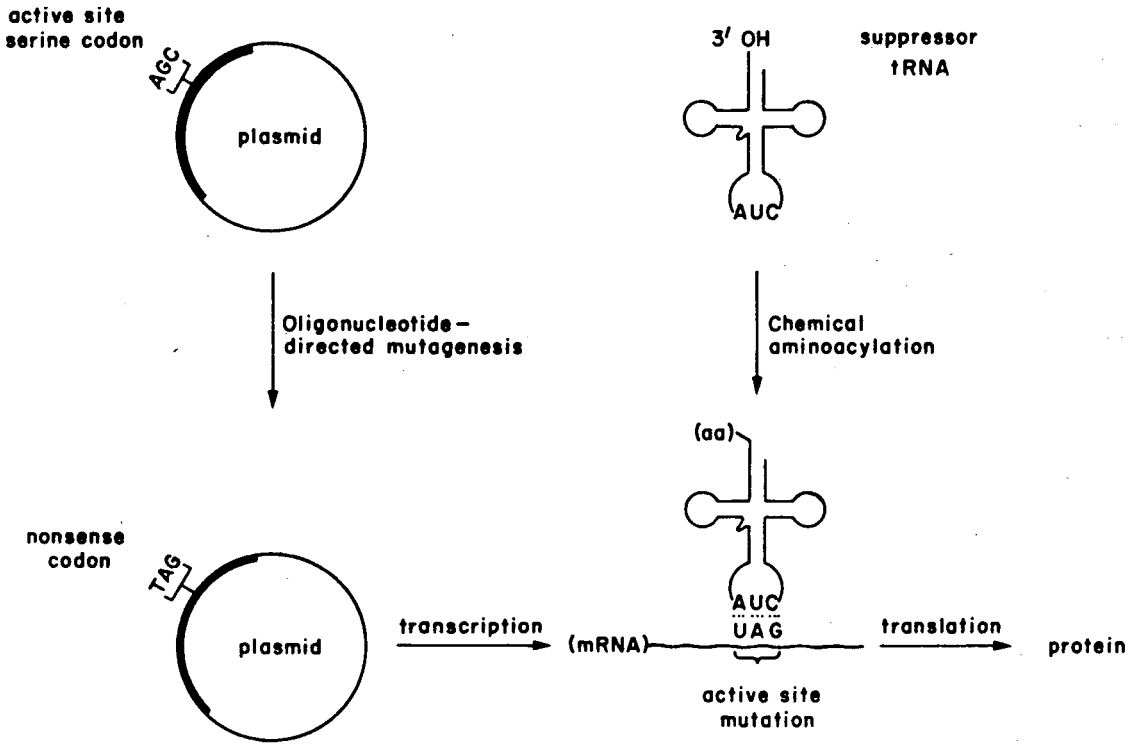

Fig. 1. Proposed scheme for introducing synthetic amino acids into predetermined sites in enzymes.

interfacial failure, and thin-film decohesion is being applied to industrially important problems of degradation of reactively formed coatings. Such coatings often have high compressive stresses from growth and can fail by buckling, delamination, and spalling. In severe cases, recurrent cycles lead to damage beyond serviceability.

The methods being developed for the study of interrelated growth mechanisms, stresses, and morphology, and of mechanisms for pore or crack formation at the interface or within the oxide, have broader applicability, e.g., to silicide films. Expected benefits include methods of improving the integrity of coatings such as oxide, boride, or nitride layers and thus of improving the prospect for increased service life of heat-, corrosion-, or wear-resistant components, where adherence between coating and substrate is essential.

Accomplishments

The stress state, morphology, microstructure, and defect population of scales and mass transport within scales are inexorably intertwined. Thus, the approach is to develop fundamental coating-formation theories addressing these issues and to apply theories for film degradation by splitting and delamination or by buckling, delamination, and cracking. Experimental evaluations of kinetics, growth stresses, and degradation mechanisms in specific cases are being correlated with film microstructures and used to refine the theories. Comprehensive models for formation, degradation, and susceptibility to mechanical damage for oxidation- and corrosion-resistant coatings should emerge from this approach.

Oxidation Theory. A two-dimensional, quasi-steady-state model developed for formation of oxide with columnar grains by boundary diffusion, in combination with prior theory development here for oxidation by volume diffusion, permits prediction of stresses arising during oxidation and of specific microstructures that ameliorate them. The oxidation rates are also predicted as in traditional theories. Generation of large stresses is often found, and important factors that control stress development during growth of oxide films are revealed.

Low-Temperature Oxidation of Copper. Thermal cycling or isothermal heating of silicon solar cells (provided by Pacific Gas and Electric Co., San Ramon, CA.) produced rapid oxidation of the electrodeposited Cu current-collecting grid, as well as very fine buckling and some spalling of the oxide film at temperatures as low as 180°C. These effects apparently ensue from the fine columnar grains and high defect content of the 10-μm-thick copper ribbons and from some Cl residue from the electrolyte. Vapor-deposited Cu (0.5–1.0 μm thick) exhibits similar rapid oxidation and spalling.

The initial oxidation rate at 180°C was more than an order of magnitude faster on deposited Cu than reported for bulk, annealed Cu. After a thickness of about 0.1 μm was achieved, the rate differences tended to diminish. The accelerated low-temperature oxidation is attributed to grain-boundary diffusion (probably of oxygen) owing to a finer grain size in these oxides compared to those in bulk metal. The finer implied oxide grain size presumably derives from microstructures of the deposited Cu, but quantitative correlations are required.

Further enhancement of oxidation results from the presence of small amounts of chloride salts on the copper surface and also appears to arise from use of intense incandescent light for heating. These observations are in keeping with reported Cu oxidation studies, but not understood.

Oxide Delamination and Degradation. Microbuckling of the oxide scale occurred when it achieved a critical thickness, about 0.3 μm. The very early onset of buckling and spalling during low-temperature oxidation of deposited Cu presumably is due to the fine, columnar grain structure that provides for enhanced oxygen diffusion and the generation of much higher compression stresses in the plane of the oxide, in comparison with higher-temperature oxidation of bulk copper.

A simple mechanics evaluation, in concert with the oxidation theories, explains several aspects of the buckling. The decohesion accompanying buckling is favorable only for a sufficient film thickness. When a published analysis for single buckles and the large stresses (2 GPa) predicted from the oxidation theory is used, the driving force for the growth and requisite decohesion of a stable buckle is predicted as $G = 5\ J/m^2$ at the observed critical thickness and for larger-than-minimum buckle sizes. This value is similar to the fracture resistance found for other ceramic-metal interfaces and seems high enough to account for stability of the buckles in the absence

of specific G_c data for the interface. The complex multiple buckling is similar to that predicted for buckling of plates on elastic foundations, but these theories do not address the concomitant decohesion. The flaws providing an initial delamination that is large enough to buckle are not identified. However, impurity accumulation at the interface may reduce the fracture energies sufficiently to allow pore formation in response to predicted stresses normal to the interface and subsequent coalescence into precursor cracks before buckling. Residual curls observed in the spalled oxide attest to gradients in the in-plane stresses; these should permit quantitative confirmation of the rapidly diffusing species and may play a role in initiating buckling.

Coating and Interface Characterization. Transmission electron microscopy of cross sections of the oxide scale showed that it was essentially Cu_20 with a grain size of about 0.1 μm but contained appreciable internal faults. In contrast to indications from the scanning electron microscopy, the grain structure was quite equiaxed for scale exceeding a micrometer in thickness; since such microstructures may reduce the growth stresses, the dependence on growth conditions merits further investigation.

Applications of the Theory of Phase Transformations

Principal Investigators: J.W. Morris, Jr. and Armen G. Khachaturyan

Funding: $29,800

Project Description

This program developed the theory of structural phase transformations in solids and applied it to the solution of practical problems in the design of new materials. Specific tasks included: (1) the prediction of coherent precipitate structures in solids; (2) the determination of the shapes and morphologies of coherent precipitates in solids; and (3) the preparation of new ceramic phases through controlled ordering on the cation lattice.

Accomplishments

Coherent Precipitates. The coherent precipitate of greatest current practical importance is the Ll_2 ordered phase on the FCC lattice. This phase has stoichiometric composition A_3B and is the structure, for example, of the γ' phase in high-temperature superalloys and intermetallics and of the δ' phase in Al-Li. The low-temperature equilibrium between a disordered solution and an Ll_2 phase was treated analytically using a mean-field model with an arbitrarily long-range binary interaction. The equilibrium phase field can be written as a function of two parameters, the mean value of the interatomic interaction V(0) and the potential of the ordering wave for the Ll_2 structure $V(k_1)$, where $k_1 = (2\pi/a)[100]$. The model was specifically applied to the Al-Li system and shown to provide a good fit to the low-temperature portion of the two-phase field. Its results explain the observed deviation from stoichiometry in the δ' phase. Initial work on the γ' phase in Ni-Al suggests that the model is applicable to this system as well.

In addition to the equilibrium phase field, the model permits a straightforward analysis of the transformation paths that may be taken when a disordered solution is quenched into the two-phase field. The predicted transformation path is a cascade of instabilities, which has never before been recognized. The disordered phase orders congruently on quenching, but the congruent ordered phase is unstable with respect to disorder. The final product of the transformation is a microstructure that contains small islands of ordered phase in a disordered matrix. These results are consistent with the transformation phenomena observed for Al-Li alloys and plausibly explain some of the apparent anomalies in the quenching behavior.

The model also allows the computation of the surface energies of antiphase boundaries in the ordered alloy and in the interfaces between the ordered and disordered phases. The resulting theory is the first to compute these energies in a form that considers interactions beyond the first nearest neighbors. The energies were computed for Al_3Li and show good quantitative agreement with the best experimental data, which has important implications for the design of high-temperature alloys.

Precipitate Morphologies. For some years, researchers have been puzzled by an apparent instability during the coarsening of cubic γ' precipitates in Ni-based superalloys. After reaching a certain critical size, the cubic precipitates decompose, first into two, and then into eight discrete particles. An interpretation

based on the mismatch in the elastic constants between the precipitate and the matrix has recently been proposed by a group at National Bureau of Standards (Cahn and co-workers). The explanation may be simply related to the elastic anisotropy of the precipitate phase, in which case it is straightforward to compute the critical precipitate sizes and the equilibrium separations of the discrete product phases. The theory has been worked out and is in excellent numerical agreement with the experimental observations on Ni_3Al. The theory also provides the criteria that determine the shapes of similar precipitates in other systems. These can be simply stated in terms of a characteristic length that is set by the elastic constants.

Tunneling Microscopy of Catalysts

Principal Investigator: Miquel B. Salmeron

Funding: $110,900

Project Description

A new scanning tunneling microscope was developed and applied to current questions in surface science and catalysis, such as the morphology of metals deposited on metals and of oxide thin layers.

Accomplishments

The first high-quality results with the recently built scanning tunneling microscope (STM) have been obtained. The first test surfaces used were selected for their inertness in air and included evaporated gold films on mica, gold single crystals, and graphite. The STM experiments were carried out in the atmosphere, but in the case of the Au(334) single crystal, the surface was prepared in ultrahigh vacuum to ensure cleanliness and to confirm the presence of an ordered monoatomic step structure with low-energy electron diffraction (LEED). The STM images in air were of high quality with a noise level in the z direction (perpendicular to the surface) of less than 0.1 Å. The resolution of the instrument in the surface plane varied in successive experiments depending on the tip diameter. The best figure was 1 Å (obtained with graphite), and in the case of gold it was typically 10 Å. It was found that the monoatomic step structure is stable in air. The lines of parallel steps form domains several thousand angstroms wide in the form of large plateaus, as shown in Figure 2. The Au films on mica, on the other hand, were found to be atomically smooth over distances of thousands of angstroms. Another interesting result obtained with the instrument is the observation of the faceting of the Au(334) surface that occurs when oxide impurities segregate to the surface as a result of heating above 500°C in air. The best performance of the instrument was obtained with graphitic carbon surfaces, where atomic resolution images were obtained, as shown by Figure 3.

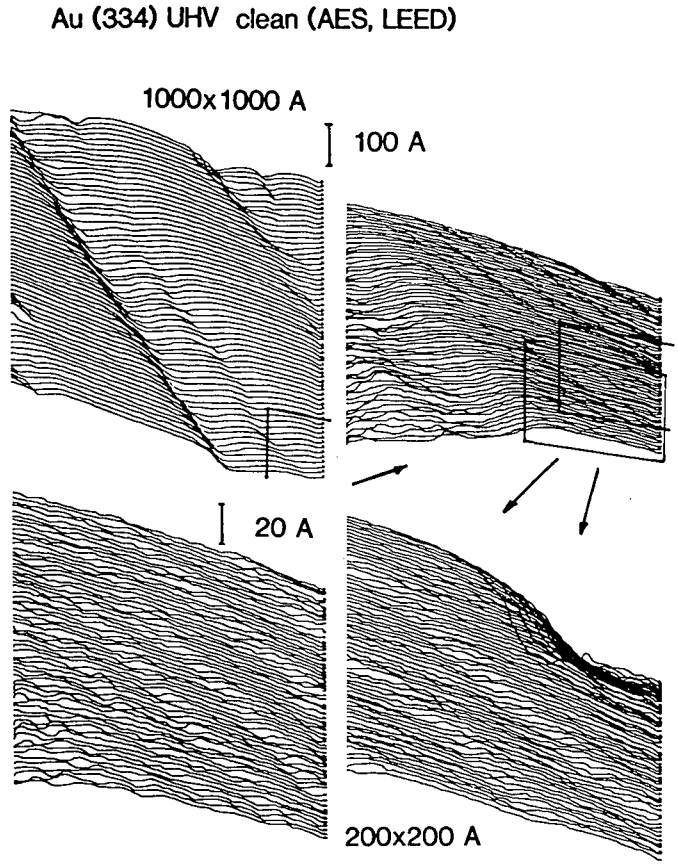

Fig. 2. Scanning tunneling microscope images of Au(334) in air. The crystal was cleaned and annealed in ultra high vacuum prior to imaging. The successive magnifications reveal the parallel lines of steps of one atom height. The imaging time was 3 minutes per frame.

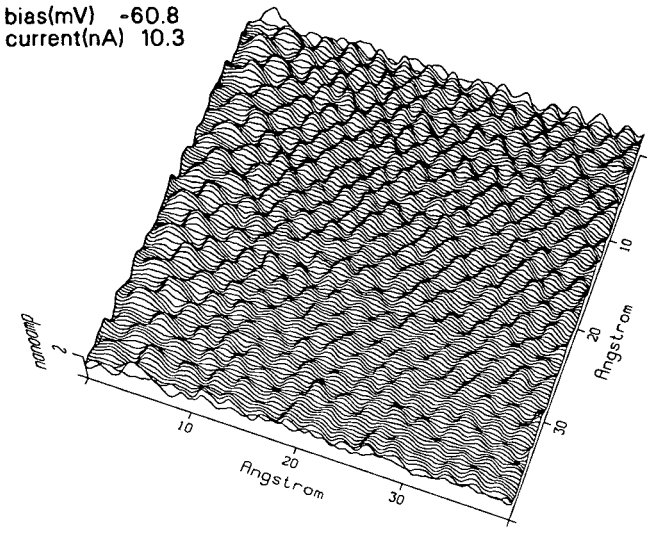

Fig. 3. Graphite surface viewed with the Scanning Tunneling Microscope in the fast scan mode (current imaging). Individual atomic bumps are observed with a periodicity of 2.4 Å. The "missing" atom of the honeycomb structure is due to the different electronic densities at the Fermi level in alternate C-atoms. Scanning time was 5 seconds.

Molecular Composites as Potential Candidate Material for Encapsulation of Integrated Circuits and Packaging Microelectronics

Principal Investigator: David S. Soane

Funding: $19,600

Project Description

This project investigates thermosets used in microelectronics encapsulation and packaging, specifically thermoelastic stress induced by expansion coefficient mismatch of the various materials involved in a packaged integrated circuit. Another objective is to explore the use of composites consisting of rigid-rod polymers molecularly dispersed in amorphous host polymers as a replacement for existing packaging materials. Molecular composites are found to have much lower coefficients of thermal expansion, making them quite compatible with the intended components, such as silicon and copper.

Accomplishment

A bending-beam apparatus with a 3-mil-thick quartz strip housed in a high-temperature oven has been designed and constructed. Slight curvature due to a thin coating on one side of the beam (~1 μm) can be detected by precision x-y-z translators. This experimental setup permits stresses as low as 10^6 dynes/cm^2 to be discerned.

A finite-element program to predict stress profiles in a package with complex internal geometries has been written. The program at present can handle only two-dimensional problems. A material-property computer program that takes into account the effects of temperature, chemistry, stoichiometry, rate of curing, viscosity, modulus, and solvent evaporation in calculating stresses in thin films has been partially finished. It runs for simple systems, but much refinement is desired. Modifications will be guided by the availability of new data from the experiment.

Phase diagrams based on Flory's theory for rigid rods in amorphous polymers have been successfully obtained. This program represents an extension of the last of a series of papers by Flory in 1978. Nonathermal interactions among the ternary components have been considered, such as rods, polymer, and solvents.

Publications

R.M. Cannon, R.M. Fisher, and A.G. Evans, "Decohesion of Thin Films from Ceramic Substrates," *Mat. Res. Soc. Symp. Proc. 54*, 799 (1986).

R.M. Cannon, "Microstructural and Chemical Aspects of the Fracture of Ceramic-Metal Interfaces," colloquium, Dept. of Metallurgy and Materials Science, Case-Western Reserve Univ. (Feb. 1986).

R.M. Cannon, "Fracture of Ceramic-Metal Interfaces," seminar, Material Sciences Dept., Brookhaven National Laboratory (July 1986).

C.N. Cronin, B.A. Malcolm, and J.F. Kirsch, "Reversal of Substrate Charge Specificity of Site-Directed Mutagenesis of Asparate Amino Transferase," submitted to *J. Amer. Chem. Soc.* (1987).

R.M. Fisher, "Role of the Critical Voltage Effect in Analytical Microscopy," *Mat. Res. Soc. Symp. Proc. 62*, 163 (1986).

R.M. Fisher, B. Martin, and R.M. Cannon, "Low Temperature Oxidation and Spalling of Electrodeposited and Vapor-Deposited Copper," *Mat. Res. Soc. Symp. Proc. 54*, 829(1986).

R.M. Fisher, J.B. Posthill, M. Sarikaya, J.A. Reimer, and M. Petrich, "Electron Optical Characterization of Amorphous SiC:H CVD Films," *Mat. Res. Soc. Symp. Proc. 69*, 153 (1986).

R.M. Fisher, "Thin Film Adherence," seminar, Lockheed, Palo Alto Research Laboratories (June 1986).

R.M. Fisher, "Thin Film Adherence," seminar, Chandler Fabrication Facility, Intel (Oct. 1986).

R.M. Fisher, "Interface and Adhesion Science Research At CAM," seminar, Physics Dept., General Motors Research Laboratory, (Oct. 1986).

A.G. Fox and R.M. Fisher, "Structure Factors and Debye Temperatures of Al-Li Solid Solution Alloys," *Acta Cryst,*. in press (1986).

A.G. Fox and R.M. Fisher, "Low-Angle Atomic Scattering Factors and the Charge Density of Beryllium," *Phil. Mag,*. in press (1986).

V. Jayaram, M.D. Thoulass, and A.G. Evans, "Determination of the Failure Criterion for Thin Films," presentation, Annual Mtg. Am. Ceram. Soc. (April 1986).

V. Jayaram, R.J. Fisher, and M. Sarikaya, "Coating and Interface Characterization," presentation, Pacific Coast Meeting, Am. Ceram. Soc. (Oct. 1986).

A.G. Khachaturyan, T.F. Lindsey, and J.W. Morris, Jr., "Precipitation of the δ' Phase in Al-Li Alloys," submitted to *Metallurgical Transactions* (1986).

M. Salmeron, B. Marchon, S. Ferrer, and D.S. Kaufman, "A Scanning Tunneling Microscopy Study of the Au(334) Surface in Air," submitted to *Phys. Rev.* B (1986).

M. Salmeron, D.S. Kaufman, B. Marchon, and S. Ferrer, "Structure and Thermal Stability of the Au(334) surface and Au(111) Thin Films in Air: A Scanning Tunneling Microscopy Study," submitted to *Applied Surf. Sci.* (1986).

Chemical Biodynamics Division

Tissue-Specific Expression of Ri T-DNA Genes in Nicotiana tabacum

Principal Investigators: James C. Bartholomew and Francesca Leach

Funding: $35,100

Project Description

The project is designed to identify cytoplasmic factors that are responsible for tissue-specific gene expression in a plant, *Nicotiana tabacum*. DNA-binding proteins may control gene activity in various tissues, from the embryo to the mature organism. Determination of the molecular characteristics of the specific DNA-protein complexes that correlate with root or leaf-specific gene transcription is instrumental. Work with promoters borne by the T-DNA of *A. rhizogenes* is being done for the following reasons. First, the pRi T-DNA has been shown to bear promoters that are specifically active in leaves or in root tissues. Second, the pRi T-DNA is a natural vector for plant genetic engineering, compatible with the regeneration of fertile plants, and it can thus be used to introduce modified genetic information into plant cells.

Accomplishments

Conditions that will allow plant protein-DNA complex formation have been tested. Tobacco root- and leaf-protein extracts have been tested for their DNA-binding capacities after separation of the proteins by electrophoresis and transfer to a nitrocellulose membrane. A number of proteins that show DNA-binding capacities have been observed, and large differences in the DNA-binding pattern of extracts from the two tissues were noted. Presently, work continues to characterize the nature of these proteins (histone, HMG, and others) and to assess the contribution of chloroplast DNA-binding proteins to the binding pattern observed in the case of the leaf extracts. Even if a major contribution in this difference comes from the leaf chloroplastic proteins, the two smaller molecular weight proteins (7 kD and 8 kD) present only in the root extract represent a true difference in the DNA-binding patterns of the proteins from root and leaf tissue. Testing is underway to determine whether this difference is due to an artifact of the extraction procedure. Both extracts are denatured by a number of techniques; however, leaf polypeptides never break down to such small components. This result, although preliminary, is the first evidence of a difference in DNA-associated proteins from two plant organs and, as such, is worth further investigation.

Proteins that bind specifically with the regulatory sequences of the root-specific and the leaf-specific T-DNA genes are also being isolated. Proteins are first isolated on the basis of their general DNA-binding capacity. To this end, protein extracts from each plant organ are run on DNA-cellulose affinity columns to fractionate proteins that show general DNA-binding capacities.

To visualize DNA-binding proteins, proteins are transferred to nitrocellulose filters and probed with nick-translated labeled DNA. The DNA sequences being used for these experiments are subclones containing the leaf-specific and the root-specific promoters of the pRiA4 T-DNA. The goal is to show that there is indeed a specificity in the recognition of each of these sequences by the two types of extracts and to identify what proteins are involved.

Defining conditions that will enhance the sequence specificity of DNA-binding proteins has been a major difficulty in the identification of sequence-specific recognition factors. Retarded electrophoretic migration of DNA complex to proteins has proven to be a useful method in detecting specific over nonspecific binding of proteins to isolated sequences; it has recently been used to identify specific transcription factors in SV40-infected cells and in oxygen-induced cytochrome expression in yeast.

Several approaches to determining the general and sequence-specific DNA-binding properties of the tobacco root and leaf proteins are being tested. These include investigating factors influencing the formation of DNA-protein complexes in solution, such as salt conditions, length of reaction and subsequent washes, and competition experiments with random-sequence DNA such as calf-thymus DNA.

Conversion of Singlet Molecular-Oxygen Electronic Excitation into Electrical Energy

Principal Investigator: Heinz M. Frei

Funding: $27,500

Project Description

The purpose of this project is to explore a new way for the efficient conversion of chemically stored photon energy into electrical energy. This is of key importance for conversion of the energy of the sun's most abundant, near-infrared quanta into useful energy, a yet-unaddressed problem in solar photochemistry. (More than half of the solar radiation at ground level lies in the near-infrared spectral range.) The goal is to demonstrate the feasibility of direct, quantitative conversion of chemically stored near-infrared photon energy into electrical energy.

Accomplishments

The approach, shown schematically in Figure 1, is based on the chemical storage of metastable $^1\Delta_g$ excited molecular oxygen $[0_2(^1\Delta_g)]$, which, when excited by near-infrared photons, combines very efficiently with acceptor molecules like aromatic hydrocarbons to form an endoperoxide (Figure: $O_2(^1\Delta_g) = {}^*O_2$, aromatic hydrocarbon = A, endoperoxide = $A{}^*O_2$). Thermal back reaction of certain endoperoxides regenerates 0_2 in the $^1\Delta_g$ excited state in high yield, opening up the possibility of directly converting its electronic energy into electrical energy (hence bypassing a Carnot cycle). This could be done by initiating an excited-state redox reaction with the thermally retrieved $0_2(^1\Delta_g)$, whose products would spontaneously regenerate the ground-state reactants. Conducted in an electrochemical-cell configuration, such a reversible excited-state redox reaction of chemically stored $0_2(^1\Delta_g)$ would permit, in principle, quantitative conversion of stored chemical energy into electricity.

Realization of this concept required development and kinetic study of singlet delta 0_2 endoperoxide storage systems in aqueous solution. Then reversible excited-state redox reactions of oxygen that permit conversion of $0_2(^1\Delta_g)$ electronic energy into electrochemical potential were explored.

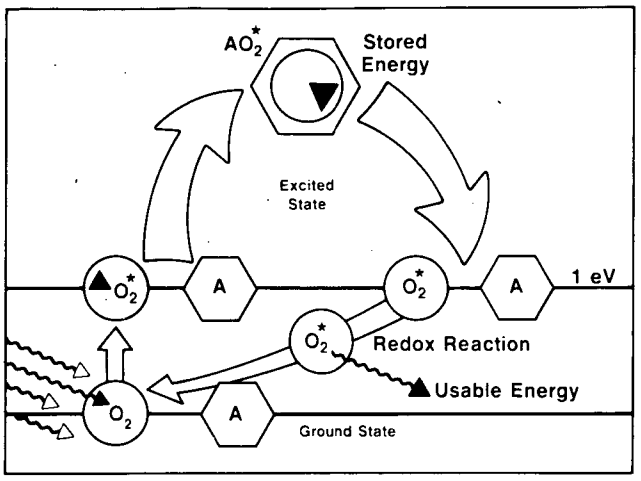

Fig. 1. Photons of near-infrared light can excite a diatomic oxygen molecule (O_2) into a higher energy state (O_2^*). The excited molecule combines with another molecule, the "acceptor" (A), to form an endoperoxide (AO_2^*) in which energy is stored. When the endoperoxide breaks down, the oxygen keeps its additional energy. A "redox" reaction to reduce the oxygen to its ground state can be used to retrieve the stored energy.

Since emphasis is on the elucidation of the mechanism of the new chemistry, processes were studied in real time by laser-flash-chemiluminescence and transient absorption spectroscopy.

This exploratory project began by synthesis and spectroscopic study of an ionic, highly water soluble, oxygen-storing molecule, 3,3′-(1,4-naphthylidene) dipropionate endoperoxide. By observation of the extremely weak, 1.3-μm, near-infrared chemiluminescence of $0_2(^1\Delta_g)$ with a very sensitive Ge detector, the first direct evidence for thermal retrieval of singlet excited 0_2 from an oxygen-storing molecule in aqueous solution was obtained. In addition to its use for singlet oxygen storage in aqueous solution, this ionic endoperoxide is ideally suited for later testing of the efficiency of direct reduction of the expelled $0_2(^1\Delta_g)$ on a semiconductor electrode surface, since its carboxy groups enable it to adsorb strongly on such a surface.

The main effort, which involved use of the near-infrared-chemiluminescence technique, was focused on attempts to monitor the fate of $0_2(^1\Delta_g)$ retrieved from this endoperoxide storage molecule

in real time. When exciting the endoperoxide in aqueous solution to the second singlet excited electronic state with a 5-nanosecond UV-laser pulse, expulsion of $0_2(^1\Delta_g)$ occurred in sufficient amount to permit time-resolved study of its subsequent decay for the first time. It was found that the decay is entirely dictated by solvent deactivation, most clearly manifested by the large factor of 15 D_20/H_20 isotope effect on the decay rate of $0_2(^1\Delta_g)$. The long (63-μs) lifetime of the retrieved singlet 0_2 in D_20 makes this an ideal solvent for the search of $0_2(^1\Delta_g)$ excited-state redox chemistry.

A search has begun for $0_2(^1\Delta_g)$ excited-state reactions that would accomplish conversion of $^1\Delta_g$ electronic energy into electrochemical potential. A very promising system, both on thermodynamic grounds and in terms of its potential realization in an electrochemical cell, is the excited-state two-electron transfer reaction:

$$0_2(^1\Delta_g) + 2H^+ + 3Br^- \rightarrow Br_3^- + H_20_2 \ .$$

In a steady-state experiment using FTIR and UV/VIS spectroscopy to follow the chemistry, it was observed that $0_2(^1\Delta_g)$ oxidizes HBr to Br_2 in nonpolar solvents like $CHCl_3$ and CCl_4. Definitive proof for $0_2(^1\Delta_g)$ excited-state chemistry was accomplished by observation of a D/H solvent isotope effect on the Br_2 project yield that reflects the deuterium isotope effect of the $^1\Delta_g$ lifetime. This is the first observation of a bromide-to-bromine oxidation by singlet oxygen. Currently, attempts are underway to observe this reaction in apolar and aqueous solvents in real time, using a nanosecond laser flash-chemiluminescence apparatus with newly added transient absorption capability.

Photosynthetic Gene Expression

Principal Investigator: John E. Hearst

Funding: $16,800

Project Description

Development of techniques for making oligonucleotides that are important in a number of projects.

Accomplishments

Construction of DNA Substrates Modified with Psoralen at a Unique Site and Study of the Action Mechanism of ABC Excinuclease on These Uniformly Modified Substrates. Psoralens bind to DNA noncovalently and, upon exposure to near UV light (320–400 nm), produce covalent adducts. Thymidine residues in DNA, especially those at 5′-TpA-3′ sequences, are most susceptible to the photochemical reaction. This property of the reaction and recent advances in oligonucleotide synthesis and separation have made it possible to construct DNA fragments containing psoralen adducts at a specific site. The octanucleotide 5′-TCGTAGCT-3′ was photoreacted (in the presence of the complementary strand) with the synthetic psoralen 4′-hydroxymethyl-4,5′,8-trimethylpsoralen to obtain oligonucleotides adducted via the furan or pyrine ring at the internal thymine. These modified octanucleotides were ligated to nonmodified oligonucleotides to obtain a 40-base-pair DNA fragment containing a psoralen adduct at a central location. The modified fragment having the thymine-furan side 4′-hydroxymethyl-4,5′,8-trimethylpsoralen adduct was irradiated with 360-nm light to produce an interstrand cross-link, and this cross-linked DNA was purified to homogeneity. These uniquely modified DNAs were used as substrates for *E. coli* ABC excinuclease to determine its incision mechanism unambiguously and to determine the contact sites of the enzyme. ABC excinuclease mediates the cleavage of the eighth and fifth phosphodiester bonds 5′ and 3′, respectively, to psoralen monoadducts, and the ninth (5′) and third (3′) phosphodiester bonds to the furan-side thymine of the cross link. Preliminary DNase I footprinting studies show that ABC excinuclease protects the whole 40-base-pair fragment from DNase I and that binding of the A and B subunits to the furan-side monoadducted substrate produces two hypersensitive phosphodiester bonds in the vicinity of the 5′ incision site of ABC excinuclease.

Action Mechanism of ABC Excision Nuclease on a DNA Substrate Containing a Psoralen Cross Link at a Defined Position. Many carcinogenic as well as chemotherapeutic agents cause covalent linkages between complementary strands of DNA. If unrepaired, DNA cross links are blocks to DNA

replication and transcription and therefore represent potentially lethal lesions to the cell. Genetic studies of *E. coli* have demonstrated that the repair enzyme ABC excision nuclease, coded for by the three unlinked genes uvrA, uvrB, and uvrC, plays a crucial role in DNA cross-link repair. To study the molecular events of ABC excision nuclease-mediated cross-link repair, a DNA fragment with a psoralen-DNA interstrand cross link at a defined position has been engineered. This substrate was digested with pure enzyme, and the reaction products were analyzed on DNA sequencing gels. It was found that the excision nuclease: (1) cuts only one of the two strands involved in the cross link, (2) incises the cross link by hydrolyzing the ninth phosphodiester bond 5′ and the third phosphodiester bond 3′ to the furan-side thymine of the cross link, and (3) does not produce double-strand breaks at any significant level. Based on these data, a model was developed in which ABC excision nuclease initiates cross-link repair *in vivo*.

NMR Studies of the Structure and Dynamics of Biopolymers

Principal Investigator: David Wemmer

Funding: $35,300

Project Description

This project is directed to several problems of protein and oligonucleotide structure using high-resolution NMR spectroscopy. The general goals of the project are to understand the solution structure of DNA molecules with a nick or gap in the sugar phosphate backbone as simple models for damaged DNA, to determine the structure of a drug/DNA complex and the microscopic kinetics of the binding steps, and to analyze the structures of several small cystine-rich proteins to enhance the understanding of the active parts of the structure. Significant effort has gone into implementating methods for preparing large quantities of specific-sequence DNA oligomers for study and into setting up the necessary software on a VAX computer system for the analysis of NMR data and the required structure calculations.

Accomplishments

Gap DNA Structures. By choosing special sequences for synthetic DNA oligomers, stable "sticky-end" dimers in solution from DNA hairpin with dangling ends have been formed. The sequences are chosen with a central section that is not complementary to any other in the molecule and that is flanked by a self-complementary sequence and a self-complementary dangling tail, which allow two such molecules to associate in solution. The imino proton spectra from these molecules confirm that such a dimer is indeed the stable form in solution. The imino resonances have been assigned using nuclear Overhauser-effect difference spectra, and they confirm that the dimer is a single continuous double helix in solution. On each of the strands, however, there is a break and a missing phosphate. Complete two-dimensional NOE data sets (NOESY spectra) of two different sequences have now been collected. The cross-peak intensities reflect the inverse sixth power of distances between protons. When the intensities of many cross peaks in the spectrum were analyzed, with particular attention paid to those at the site of the gap in the backbone, it was determined that the backbone is relatively undistorted, as compared to a standard "B DNA," even at the site of the gap. There is a slight overwinding of the DNA at this site, giving a slightly greater than average local helix twist angle. The temperature dependence of the NMR spectrum has also been used to examine the melting in these sequences. Melting occurs first as a separation of the dimer into monomers, followed at higher temperature by opening of the hairpin loop. For sequences with four GC base pairs in the overlap region and six in the stem of the hairpin loop, these melting events are separated by about 15°C, with the first transition having slower exchange kinetics between monomer and dimer than the latter.

DNA-Drug Binding. NMR studies of the binding of the antibiotic distamycin-A to a specific DNA dodecamer have previously been conducted. This drug shows a strong preference for binding at AT-rich sequences (AATT in the cases studied in detail). From the NMR data it was possible to position the drug relative to the DNA and to qualitatively evaluate the degree of distortion of

the DNA by the drug. These measurements have now been supplemented by energy-minimization calculations carried out with the AMBER program. A general problem with such calculations is that the minimization algorithm cannot find a global minimum of energy in a reasonable time. However, when the calculation is started near the experimentally determined structure, the energy obtained upon convergence is lower than when starting from other structures. The coordinates obtained through such experimentally guided modeling are better than those that can be determined from the NMR data alone. Extension of the measurements to other DNA sequences, to compare binding constants and the kinetics of drug binding, is now underway.

Analysis of Protein Structures. The use of cystines at specific locations in proteins to fold predictably the remainder of the sequence is of interest. The expectation that this will occur is based upon the observed folding in several naturally occurring peptides, which have common cystine positions. The resonances in two of these peptides have been previously assigned and their secondary structure qualitatively modeled. A more quantitative analysis is now being carried out. To do this, two-dimensional NOE spectra and integrated cross-peak intensities have been collected to obtain interproton distances for apamin, a small neurotoxic peptide from honey-bee venom. Distance-geometry calculations have been carried out with a relatively large number of such distances. This approach takes the distance estimates, including estimates for the experimental precision, and computes coordinates for structures that are consistent with all of the input data. Structures obtained from repeated calculations can be analyzed to give an effective "resolution."

Analysis of the relationship between structure, function, and immunogenicity of protein toxins isolated from sea anemones has been initiated. These again have common cystine positions and several other conserved residues, but different toxins are active against different receptors and do not all show antibody cross reactivity. Resonances of the RpII toxin have now been fully assigned, and it has been established that its only regular secondary structure is beta sheet, with strands connected with a variety of loops and turns. From the refined structures for proteins in a related family such as these, common structural features that give rise to similar folding of the peptide chain will be sought, while also seeking the differences leading to different activities and immunogenicity (Figure 2).

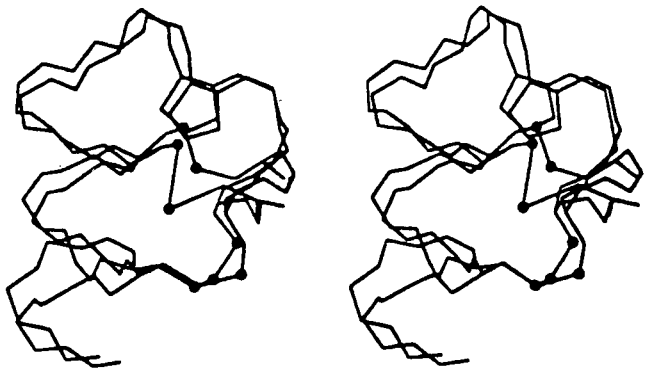

Fig. 2. Two structures of the peptide apamin are shown, which were determined from NMR data. Stereo drawings are shown of the backbone atoms, with sulfur positions indicated with circles.

Publications

P.T. Chou, S. Khan, and H. Frei, *Chem. Phys Lett. 129*, 463 (1986).

B. Van Houten, H. Gamper, J.E. Hearst, and A. Sancar, *J. Biol. Chem. 261*, 14135 (1986).

B. Van Houten, H. Gamper, S.R. Holbrook, J.E. Hearst, and A. Sancar, *Proc. Natl. Acad. Sci. USA 83*, 8077 (1986).

Earth Sciences Division

Removal of Selenium from Groundwater

Principal Investigator: Oleh Weres

Funding: $29,300

Project Description

The Kesterson Reservoir in Merced County, California, is a storage and evaporation facility for agricultural drain water, which about five years ago was found to be contaminated with selenium. Research has demonstrated that very little selenium is transported to the shallow aquifer below the ponds by the percolating pond water. Most of the selenium is removed from the pond water by, and retained in, the top few inches of pond-bottom sediment, which is rich in decaying organic matter. This same process was tested in the laboratory as a possible means of water treatment to remove selenium.

Accomplishments

Experiments done in small glass columns have established that selenium is, in fact, removed from drain water that is allowed to percolate through pond-bottom sediment from Kesterson Reservoir. Unfortunately, the nitrate in the water oxidizes the sediment, ultimately destroying its ability to sequester selenium. Adding glucose to the water protects and enhances the sediment's ability to sequester selenium. However, duplication of the reservoir process by using glucose or other organic matter in an external system would be impractical. Ecological work at Kesterson Reservoir has demonstrated that the deep-water ecosystem there is highly productive. In principle, vegetation growing in those ponds should supply enough organic matter to maintain anaerobic conditions in the sediment.

The complete process, including algae culture, has been successfully demonstrated in an outdoor 30-inch column for six weeks. At percolation rates of 50 and 100 feet per year, selenium removal averaged 94%, with 2% conversion to dimethyl selenide. An average percolation rate of 50 feet per year would allow the entire water treatment requirement of the San Luis Drain to be satisfied by a 160-acre pond (Figure 1). This process is very simple and may prove very economical. It is "appropriate technology" that any large farmer or irrigation district should be able to build and operate. It lends itself to installations of widely varying capacity, including single-farm or even single-field treatment units.

An inverse relationship between nitrate loading and selenium removal was also observed at Kesterson Reservoir. Extensive breakthrough of selenium to deep groundwater was observed only in the area of direct application of drain water. That area experienced the highest nitrate concentrations and percolation rates, and nitrate

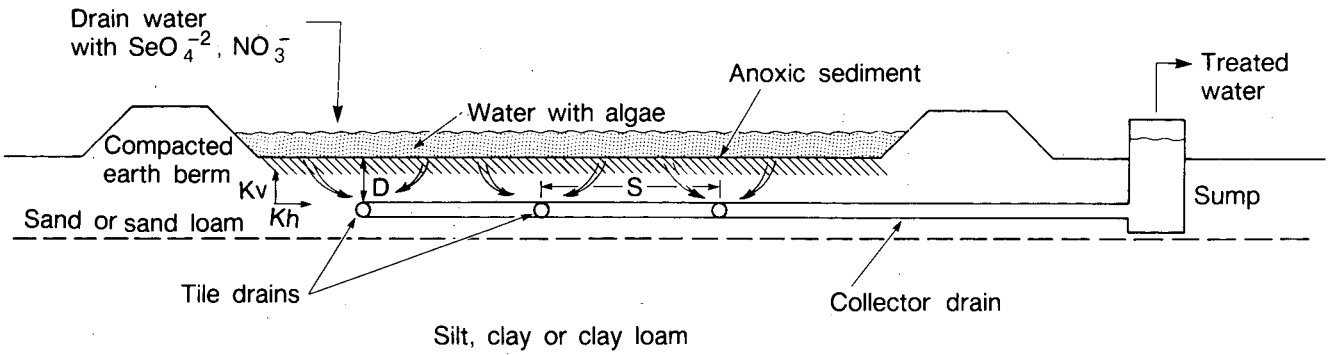

Fig. 1. Possible design for a water treatment pond designed to remove nitrate and selenium from agricultural drain water. Tile drains are seen end-on.

overwhelmed organic matter in the sediment, allowing selenium and nitrate to break through to the groundwater. Selenium in groundwater was always found in association with nitrate, and nitrate with selenium.

Design and Development of a Downhole Shear and Compressional Wave Source

Principal Investigators: Paul A. Witherspoon, Neville G. W. Cook, Michael A. Green, Kenneth F. Mirk, Ernest L. Majer, Thomas V. McEvilly and Larry R. Myer

Funding: $120,900

Project Description

This project involved the design and development of an innovative downhole shear and compressional seismic-wave source. The device will have wide application in petroleum and geothermal reservoir studies, toxic- and nuclear-waste disposal-site investigations, and many other studies requiring subsurface imaging or acoustic tomographic reconstruction of rock-mass characteristics. The device is capable of generating shear (*S*) waves of two polarizations and compressional (*P*) waves over the frequency range of 0.1 kHz to 1 kHz, and will rely on the swept frequency signal principles for analysis by correlation techniques commonly used in seismic exploration. The goal is a working prototype borehole tool proving the concept and demonstrating the potential for producing a unit with an effective signal range of 1 km and an operating depth of 5 km.

Investigations led to the conclusion that the proposed device can readily be divided into four component parts for purposes of design and preliminary testing. These four parts are: (1) *S*-wave source with axial vibratory motion; (2) *S*-wave source with torsional/rotational vibratory motion; (3) *P*-wave source with radially directed vibratory motion; and (4) borehole clamp.

Accomplishments

Linear Axial *S*-Wave Generator. Conceptual design studies were completed, a complete set of engineering drawings produced, and principal components fabricated for the *S*-wave source with vibratory mode parallel to the axis of the borehole. The design concept for this device is illustrated in Figure 2, which is a schematic cross section of the central portion of the unit. The vibratory motion is produced by interaction of the coil with the magnetic field produced by samarium cobalt magnets mounted on the core. The magnets are radially magnetized so that the magnetic flux lines are perpendicular to the direction of the current flowing in the coil. The magnetic circuit is completed through the housing and the central core. Vibratory motion of the same frequency can be attained by applying an alternating current to the coil. A symmetric component configuration was chosen as shown in Figure 2 with each magnet-core assembly holding five ring magnets. With an input power of 700 W, the total static force output of the

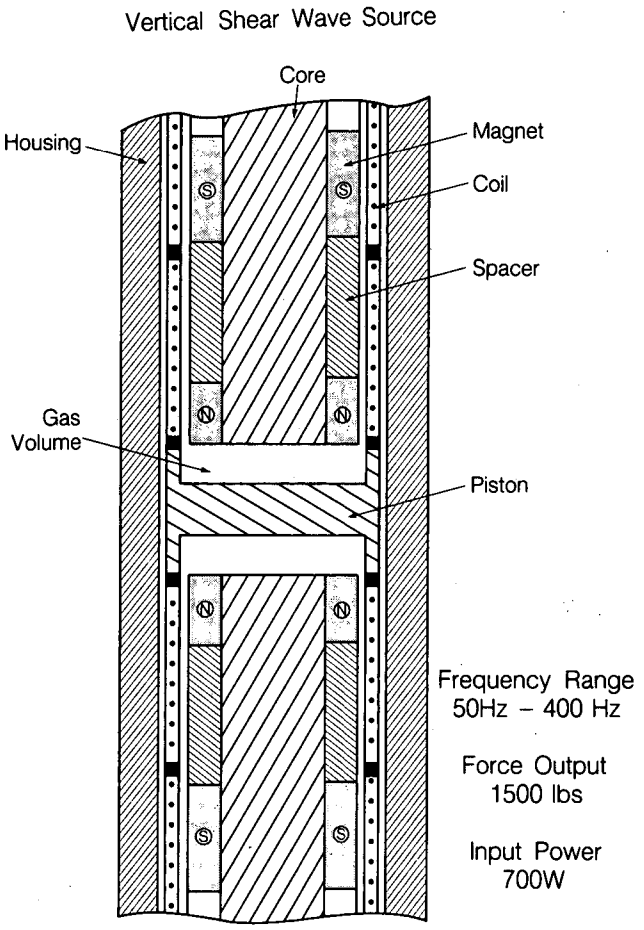

Fig. 2. Schematic cross section illustrating design concept for linear axial S*-wave source.*

magnet-coil system was calculated to be about 150 lb. To increase the force transmitted to the borehole wall, a design that enabled the device to operate in a resonant condition at all frequencies was adapted. After a reasonable damping factor was assumed, a peak force output of 150 lb was calculated for the configuration described above.

The key element of the design that permits variable frequency resonance is a pneumatic spring of variable stiffness. The spring action is provided by compression of the gas volume, as shown in Figure 2. As the coil-piston assembly moves, the gas is compressed. The resistance of the gas to compression translates into a force that acts on the core-magnet assembly and is ultimately transmitted to the borehole wall. Varying either the volume of gas or its pressure results in a change in the stiffness of the pneumatic spring. The stiffness is adjusted to achieve resonant motion of the coil-piston assembly as the driving frequency is swept over the desired bandwidth.

In FY 1986, the coil-piston assembly, magnet-core assemblies, housing, and housing extension were fabricated. The housing extension will contain instrumentation that must be carried downhole with the unit. The overall dimensions of the unit, excluding clamp, are 63 inches in length by 5 inches in diameter.

Torsional *S*-Wave Source. The concept of a torsional (*SH*) source was tested by fabricating a bench model using two DC 12-V motors and a 100-A power supply. The purpose is to measure the amount of energy (efficiency) produced by driving a reaction mass with the two DC motors. This bench model showed promise, and plans proceed to use high-output permanent-magnet motors at speeds up to 20,000 rpm. A second concept for the torsional source uses a rotating variable-mass system to drive asymmetric masses in the borehole at variable speeds to sweep over a particular frequency range. Preliminary design calculations indicated that this method may be the best solution for the torsional source.

***P*-Wave Source**. The conceptual design has been completed for a device that will generate controlled compressional waves on the wall of a borehole. The *P*-wave generator uses two linear motors arranged so that the axial motion of the two armatures is in opposition. The oscillating reaction forces generated in the stators of the two motors will drive opposing hydraulic cylinders. The resultant pressure variations can be applied to a fluid reservoir that is firmly attached to the borehole casing, thus creating a pure radial *P*-wave. The magnitude of the power-supply current, and thus the amplitude of the pressure wave, can be varied over a wide, but as yet unknown, frequency range.

Borehole Clamp. For any of the above *S*-wave and *P*-wave generators to propagate seismic waves for practical distances through rock, the devices must be connected rigidly to the metal surface of a cased borehole or to the rock wall in uncased holes. This will be done using a hydraulically actuated device that expands metal arms and pads against the walls of the casing with the required force. A preliminary design incorporating three arms oriented 120 degrees apart has been completed. This clamp will be fabricated as a separate unit so that it may be attached to any of the seismic-wave generators.

Development of Industrial Support. Contacts with members of the petroleum industry, in several instances at their initiative, indicate that despite the current economic difficulties due to the drop in oil prices, there is very great interest in the development of a downhole shear and compressional seismic-wave source. Naturally fractured oil reservoirs are a common occurrence all over the world, and these complex rock systems are not well understood by the petroleum experts despite the considerable research efforts of the major oil companies. The economic importance of understanding such rock systems becomes quite evident when one considers the problem of evaluating the results and commercial potential of the first exploratory wells from an offshore platform. The platform can cost $500 million or more, and the operating costs can be $100,000 per day. Obviously, under these circumstances, any device that can improve one's ability to explore and evaluate a fractured-rock system that may contain several billion barrels of oil has an enormous economic value. Furthermore, petroleum resources for the future will more and more be found in previously-ignored fractured (as opposed to porous granular) reservoir rocks. To explore the level of interest of the oil industry in the downhole device under development at LBL, various members of the group have had conversations with research

personnel at Amoco Production, Chevron Research, Continental Oil Company, Mobil Research and Development Corporation, Phillips Petroleum Company, Shell Development Company, and Texaco Oil Company. In every case interest is great. Those companies that have testing facilities with instrumented boreholes (Amoco, Chevron, and Continental) want to help by making their facilities available for downhole testing of the devices that are now being built. Once a prototype for a shear wave source has been demonstrated, a collaboration could be pursued between DOE and the petroleum industry.

Publications

O. Weres, H. Bowman, E. Smith, L. Tsao, and W. Harnden, "Percolation Ponds for Removing Selenium and Nitrate from Agricultural Drain Water," Lawrence Berkeley Laboratory PUB-5180 (1986).

O. Weres, H.R. Bowman, E.C. Smith, L. Tsao, and W. Harnden, "Nitrate and Organic Matter Control the Adsorption of Selenium in Water Treatment and at Kesterson Reservoir," LBL-23499 draft.

Engineering Division

A New Compton Densitometer for Measuring Pulmonary Edema

Principal Investigators: Billy W. Loo and Frederick S. Goulding

Funding: $75,900

Project Description

The objective of this work is to develop a lung-density monitor using Compton scattering of gamma rays. The measurement of the absolute density of a selected portion of the lung can be used to detect the presence of, and quantify the severity of, pulmonary edema. Such a non-invasive monitor that is accurate, easily portable, safe, and inexpensive is needed for clinical use. A unique means of making accurate measurements despite the presence of the problematic chest wall has been developed. This study is directed toward proof of the basic principles and determination of an optimum system geometry through detailed experimentation. Since a practical gamma-ray source must meet many stringent requirements, problems of selecting a suitable one are addressed.

Accomplishments

A HPGe detector system has been fabricated, and a 5-mCi Ce^{139} gamma source has been acquired to conduct a series of model studies. Figure 1 depicts a typical experimental setup in which a uniform region of the lung is simulated by blocks of foam plastic of known densities and the chest wall represented by sheets of plastic placed in the entrance and exit beams. The incident beam makes an angle ϕ with respect to the frontal plane of the detector. The HPGe detector (35 mm diameter by 17 mm thick) measures the energies of the scattered photons from a collimated beam of incident photons at 166 keV. A lead shield with a recessed rectangular opening (6.4 mm wide by 19.1 mm tall) is placed in front of the detector to define the mean scattering angle θ and to suppress multiply scattered photons. A typical energy spectrum is illustrated in Figure 2, in which six regions corresponding to scattering from six target volumes at 1-cm intervals along the incident beam are identified. A background subtraction is performed by linear interpolation from counts in regions I and II near each end of the spectrum.

It was found that within certain ranges in θ and ϕ, N (the scattered count rate per unit distance along the incident beam) decreases exponentially with depth X. Thus $\ln N = C + KX$. A striking result is that the negative slope, K, is insensitive

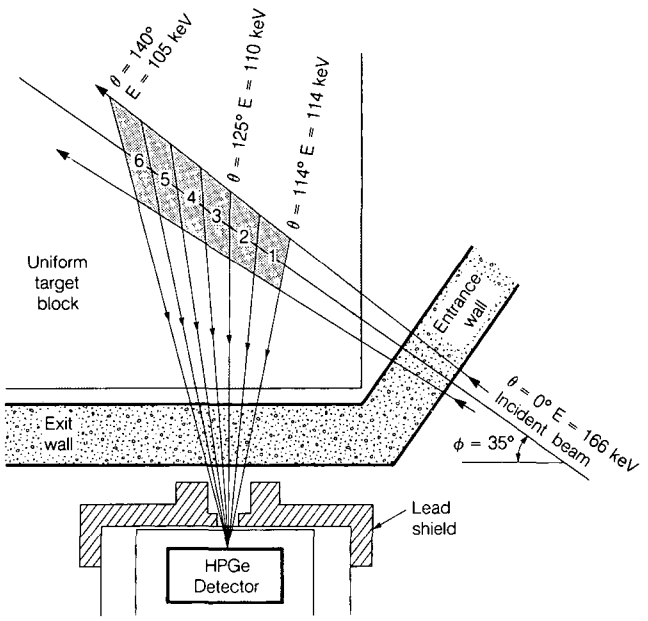

Fig. 1. Schematic of an experimental setup of the Compton backscattering geometry.

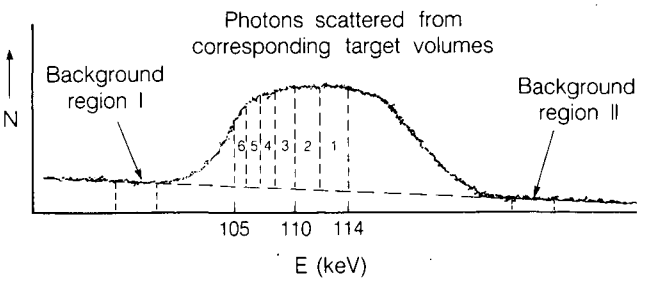

Fig. 2. Typical energy spectrum of the scattered photons.

to the presence of the chest wall, which tends to affect only the absolute count rate. It was also found that, within the range of specific gravities from 0.15 to 1.0, the value of K is a sensitive and linear function of target density ρ. Thus calibration curves such as those shown in Figure 3 allow absolute lung-density measurements unhampered by the chest walls, which have been a serious problem in earlier designs of lung-density measuring systems using gamma rays.

Table 1 summarizes some performance characteristics of the system. Measurements were first made without any plastic absorber to determine K_0. Insertion of the 19-mm-thick plastic typically reduced the count rates by a factor of two, but the new values, K_1, differed very little from K_0. The corresponding differences in density measurements $\Delta\rho$ between these two cases were calculated according to the calibration curves. Results showed that when the system configurations were changed, as ϕ was increased from 25 to 45 degrees, there were significant improvements in accuracy (especially at lower target densities) and slight improvements in sensitivity. It was concluded that with a source of about 1 Ci (37 GBq), it should be possible to make an accurate lung-density measurement in one minute, with a radiation exposure to the patient a thousand times smaller than that from a typical chest x ray.

The gamma-ray source to be used in the Compton densitometer must satisfy a large number of

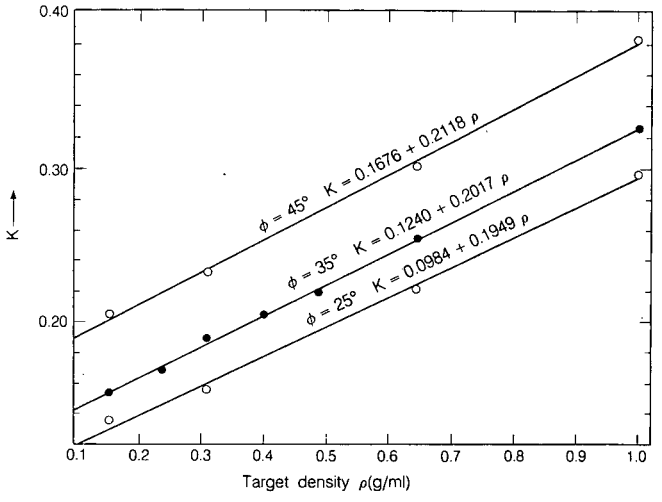

Fig. 3. Calibration curves for various system geometries relating the slope K of the counting curves to known target densities.

Table 1. Results of laboratory tests for different system geometries.

ϕ	ρ(g/ml)	0.156	0.311	0.644	1.00
25°	K_0	0.1341	0.1541	0.2207	0.2960
	K_1	0.1466	0.1661	0.2297	0.2994
	K_1/K_0	1.093	1.078	1.041	1.011
	$\Delta\rho$(g/ml)	0.064	0.062	0.046	0.017
35°	K_0	0.1533	0.1892	0.2541	0.3251
	K_1	0.1611	0.1929	0.2539	0.3299
	K_1/K_0	1.051	1.020	0.999	1.015
	$\Delta\rho$(g/ml)	0.039	0.019	-0.001	0.024
45°	K_0	0.2047	0.2313	0.2988	0.3829
	K_1	0.2088	0.2326	0.2974	0.3758
	K_1/K_0	1.020	1.006	0.995	0.981
	$\Delta\rho$(g/ml)	0.019	0.007	-0.007	-0.034

requirements from the standpoints of system performance and feasibility of large-scale production at reasonable costs. Ideally it should be a monochromatic source in the range of 100–200 keV. At higher energies, there will be increasing problems with efficiencies of the typical Ge detectors used and difficulties in providing adequate source shielding. At lower energies, there are problems with increased photoelectric absorption by chest walls, the inadequacy of detector resolution for the narrow energy range of Compton backscattered photons, and the interference of K x rays from common collimator materials such as Pb and Ta. Furthermore, the principal line should have no significant companion lines that would result in overlapping Compton-scattered spectra in the 90- to 180-degree range. The presence of high-energy (>500-keV) lines even at relatively very low intensities can significantly raise the detector background without very clumsy shielding.

In a practical clinical system, a source of about 1 Ci with a reasonable half-life (>100 days) is needed. The source material should have sufficiently high specific activity (>10 Ci/g) to form a well-collimated beam without excessive self-absorption. Finally, if the instrument is to become widely used, it must be feasible to

produce sources on the order of 10^3 Ci/year with a cost of well under $10 k/Ci. This last requirement eliminates all accelerator-produced sources, leaving those with reactor-produced sources (neutron activation) as the only candidates.

The choices have been narrowed to two radionuclides: Te^{123m}, which has a half-life of 120 days, is ideal but may have a high burn-up cross section that can limit the ultimate specific activity achievable. An alternative is Ce^{141}, which can meet all the requirements except for its shorter half-life at 32.5 days. Experiments are being conducted in collaboration with staff members at the Idaho National Engineering Laboratory and the Brookhaven National Laboratory to address the problem of producing a practical gamma-ray source.

Publications

B.W. Loo, F.S. Goulding, and D.S. Simon, "A New Compton Densitometer for Measuring Pulmonary Edema," *IEEE Transactions on Nuclear Science NS-33*, No. 1, 531-536 (1986).

B.W. Loo and F.S. Goulding, "Method and Apparatus for Measuring Lung Density by Compton Backscattering," U.S. patent filed on October 17, 1985; patent is currently being revised.

Materials and Molecular Research Division

Fundamental Aspects of Particulate Composite Structural Ceramics

Principal Investigator: Lutgard C. De Jonghe

Funding: $91,600

Project Description

Ceramic/ceramic composites offer the opportunity of combining the desirable aspects of two different materials, either of different chemical composition or of different microstructure, in one structural component. The purpose of this program is to investigate fundamental aspects of processes and parameters that control the development of properties and microstructure of particulate ceramic/ceramic composites for structural applications and to find ways in which these composites can be produced. Both colloidal processing and sol-gel methods are examined.

The approach of the project is to examine the stability and phase behavior of colloidal suspension from a theoretical point of view and attempt to produce active powders of zirconia and mullite containing dispersed second phases by sol-gel methods or by carboxylate reactions.

Accomplishments

Fabrication of monosized zirconia powders by extraction from loaded salt solvents with accompanying hydrolysis was attempted. Particles ranging between 0.5 and 5 micrometers were produced. The spread in particle sizes was significantly affected by the choice of co-solvated carboxylates. Addition of potassium salts gave the best results to date. Kinetic studies indicated that hydrolysis, leading to the formation of the zirconia, proceeded to more than 90% completion in 30 minutes at 200°C. Mullite powders prepared from hypercritically dried gels were sintered to a full dense mullite at temperatures below 1200°C. This is the lowest temperature at which such densification has been reported. Hypercritically dried powders thus may provide a means of obtaining free-fired, dense ceramic matrix composites.

Progress was made in the study of phase stability and the behavior of colloidal assemblies of particles. Solid/liquid and hexagonal/cubic phase changes could be predicted. Calculations were pursued for the determination of the effective free energy of electrically interacting colloidal particles in a finite, closed system.

Raman Studies of Surface Processes

Principal Investigator: Gerd M. Rosenblatt

Funding: $191,100 (second year of funding)

Project Description

Unenhanced spontaneous Raman spectroscopy was used to gain new understanding of the vibrational energy levels, composition, and reactivity of films and interfaces.

Accomplishments

The sample holder, sample temperature control, sample imaging, and ultra-high-vacuum systems are being completed, and integration with the Raman spectroscopy system is proceeding. The Raman spectroscopy system was characterized and used in the following studies.

Use of an Imaging Photomultiplier Tube in Raman Spectroscopy. The Raman spectroscopy system, designed and built at LBL, combines true photon-counting sensitivity with imaging detection and software by using an imaging photomultiplier tube detector. This combination results in spatially resolved spectra with multichannel detection in both the frequency and spatial regimes. Sensitivity is illustrated by examination of the O_2 fundamental (1350–1750 cm^{-1} region in air; Figure 1), which reveals: (1) the $^{16}O^{18}O$ Q-branch at 1513 cm^{-1} (this band has not been reported previously in air; the $^{16}O^{18}O$ species is 0.2% of normal oxygen) and (2) the ν_1 fundamental of CO_2 at 1389 cm^{-1} (CO_2 is nominally present in the atmosphere at 330 ppm). The spectrum acquisition time was 46 seconds with a laser power of 1 watt. These weak bands are not

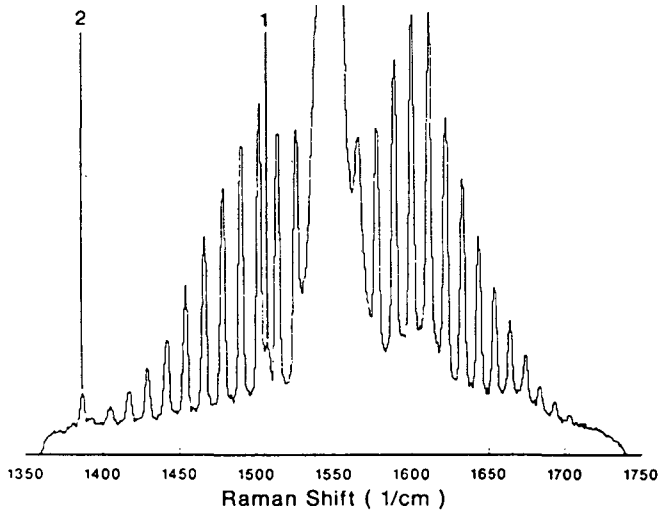

Fig. 1. Raman spectrum of air, 1350–1750 cm^{-1} region. The main feature is the Q-branch vibrational spectrum of $^{16}O_2$. The scale has been enlarged (~100x) to emphasize the O- and S-branch rotational lines. The $^{16}O^{18}O$ Q-branch, at 1513 cm^{-1}, seen as a shoulder on the O(9) rotational line, is labeled 1. The ν_1 Q-branch of CO_2 at 1388 is labeled 2.

observable in a companion experiment using a more conventional intensified photodiode array detector under the same experimental conditions. Surface Science Laboratories (manufacturer of the resistive anode used in the detector) plans to market a commercial Raman spectroscopy system based on the imaging photomultiplier tube and the systems approach and software developed by this project.

Study of Carbon Overcoats on Hard Disks. The Raman apparatus has been used to study the chemical morphology of 180-Å-thick amorphous-carbon films used as protective overcoats on hard disks. This study (in collaboration with D. B. Bogy at UC Berkeley) was motivated by questions concerning the mechanism of hard-disk failure. From the amorphous-carbon Raman spectra it was found that: (1) the Raman techniques implemented are sensitive to carbon present as a 180-Å-thick film, and (2) shifts and broadening of the carbon Raman peaks as a function of disk manufacture and treatment history reveal small differences in bonding (Figure 2).

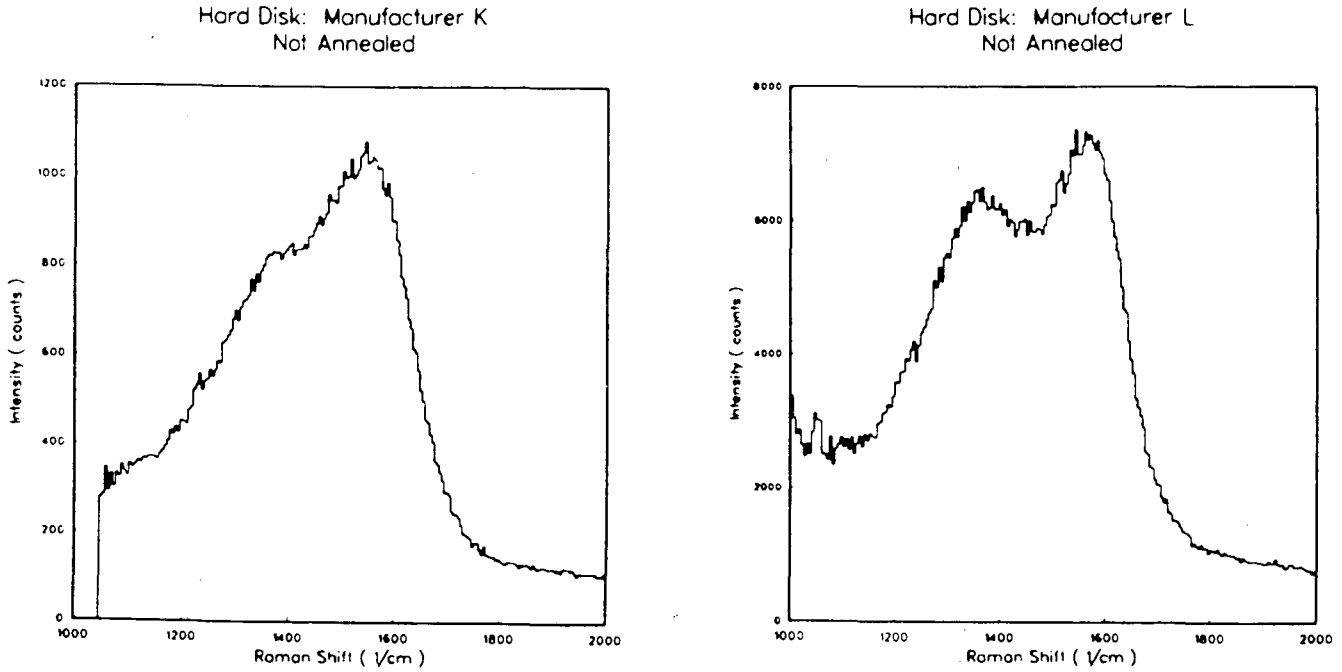

Fig. 2. Raman spectra of carbon overcoats on rigid magnetic media (hard disks), 1000–2000 cm^{-1} region. The peaks at 1350 cm^{-1} and 1565 cm^{-1}, seen in the spectra of manufacturer L, are broad and shifted from graphite, indicate of an amorphous carbon film. The further broadening of these peaks to a single broad peak, as seen in the disk from manufacturer K, indicates a "diamond like" carbon film with improved properties, i.e., increased hardness and electrical resistivity.

Structure Determination at the Metal/Solution Interface by Total Reflection Bragg Diffraction

Principal Investigators: Philip N. Ross, Jeffrey B. Kortright, and Michel A. Van Hove

Funding: $68,500

Project Description

Proof-of-principle experiments for the determination of structure at the metal/solution interface, specifically addressed to the understanding of epitaxial growth during the electrolytic deposition of metals and semiconductors, were conducted.

Accomplishments

Experimental. Because of the grazing incidence of the x-ray beam, the macroscopic optical flatness of the single-crystal surface is a prerequisite. Gold surfaces were chosen for the initial experiments because of their relative inertness (they remain clean when exposed to most gases) and the general interest in gold electrodes in physical electrochemistry. An optical table was assembled for quantitative measurement of light scattering from surfaces at grazing incidence (less than one degree). Au(111) and (100) single crystals were mechanically polished and then electropolished. It was easily established from the light-scattering measurements that the electropolished bulk crystals did not have sufficient optical flatness to be used in these experiments. It was then decided to use epitaxial gold films on cleaved mica as the surface for study, since there were many reports in the literature that clean, well-ordered flat (111) surfaces can be prepared by the evaporation of gold onto cleaved mica. The ultra-high vacuum (UHV) system was modified for gold evaporation onto a heated mica substrate, and a transfer system was built for drawing the sample out of the UHV system and storing it in argon in a glass ampule. The grazing-incidence diffraction experiments were performed during two shifts of beam time on the EXXON/LBL Beamline VI at SSRL.

The structure of the Au(111) epitaxial films was examined in UHV using low-energy electron diffraction (LEED). As prepared by evaporation, the surfaces had a high level of carbon contamination and produced a diffuse-ring diffraction pattern. After ion bombardment and thermal annealing cycling, clean surfaces were obtained, and the LEED pattern changed to a hexagonal pattern with diffuse spots. Sharp LEED patterns with super-lattice spots indicating formation of the 3×22 reconstructed surface were observed only after repeated ion bombardment and thermal annealing cycling.

The samples were removed from UHV and sealed in an argon atmosphere in glass ampules for transfer to the diffractometer at SSRL. After several days of storage in argon, the glass ampules were broken, and the samples were transferred back into the UHV system for analysis by LEED. The LEED patterns were still sharp, with the reconstructed superlattice spots clearly discernible, so there was a positive indication that this method of sample handling should preserve the surface structure.

The annealed Au (111) epitaxial films were analyzed on Beamline VI at SSRL using a grazing-incidence diffractometer borrowed from P. H. Fuoss at Bell Laboratories. As they were mounted on the diffractometer, the samples had considerable exposure to the atmosphere, something which had not occurred when the samples were transferred back into our LEED apparatus. The stability of the surface reconstruction in the atmosphere is not known. The critical angle for total reflection was measured experimentally, and subsequent scans were made both near to and far from the critical angle to obtain information about the bulk structure of the films. There is a mosaic bulk structure in these films, typical of spiral growth of dislocations, and it was possible to observe an interesting depth dependence to the mosaic structure by variation of the angle of incidence of the x-ray beam; e.g., the mosaic spread becomes narrower closer to the interface. What might be superlattice spots were observed near the <220> bulk reflection, and numerous scans were taken (seventy in all) to confirm the observation of the reconstructed surface. The results were analyzed later back at LBL.

The analysis of the experimental data began with the establishment of a correlation between the x-ray diffraction pattern and existing LEED and atom diffraction patterns. This involved, in particular, translating the three-dimensional Bragg diffraction notation to the corresponding two-dimensional notation favored at surfaces. In this

process, an earlier analysis by Ian Robinson showed that the conventional three-dimensional description of x-ray diffraction has to be amended to account for the absence of strict lattice periodicity perpendicular to the surface was verified. There result so-called truncation rods, which correspond to a smearing out of the diffraction spots in the direction perpendicular to the surface. The equivalent concept in LEED is the familiar peak broadening in intensity-voltage curves. The understanding of this point is critical to relating x-ray diffraction to the other surface-diffraction methods.

It was then possible to identify the x-ray diffraction scans in which the reconstruction of the Au(111) surface could be detected. The resulting map of reciprocal space is shown in Figure 3. The most important scan for observing the reconstruction is the in-plane scan from

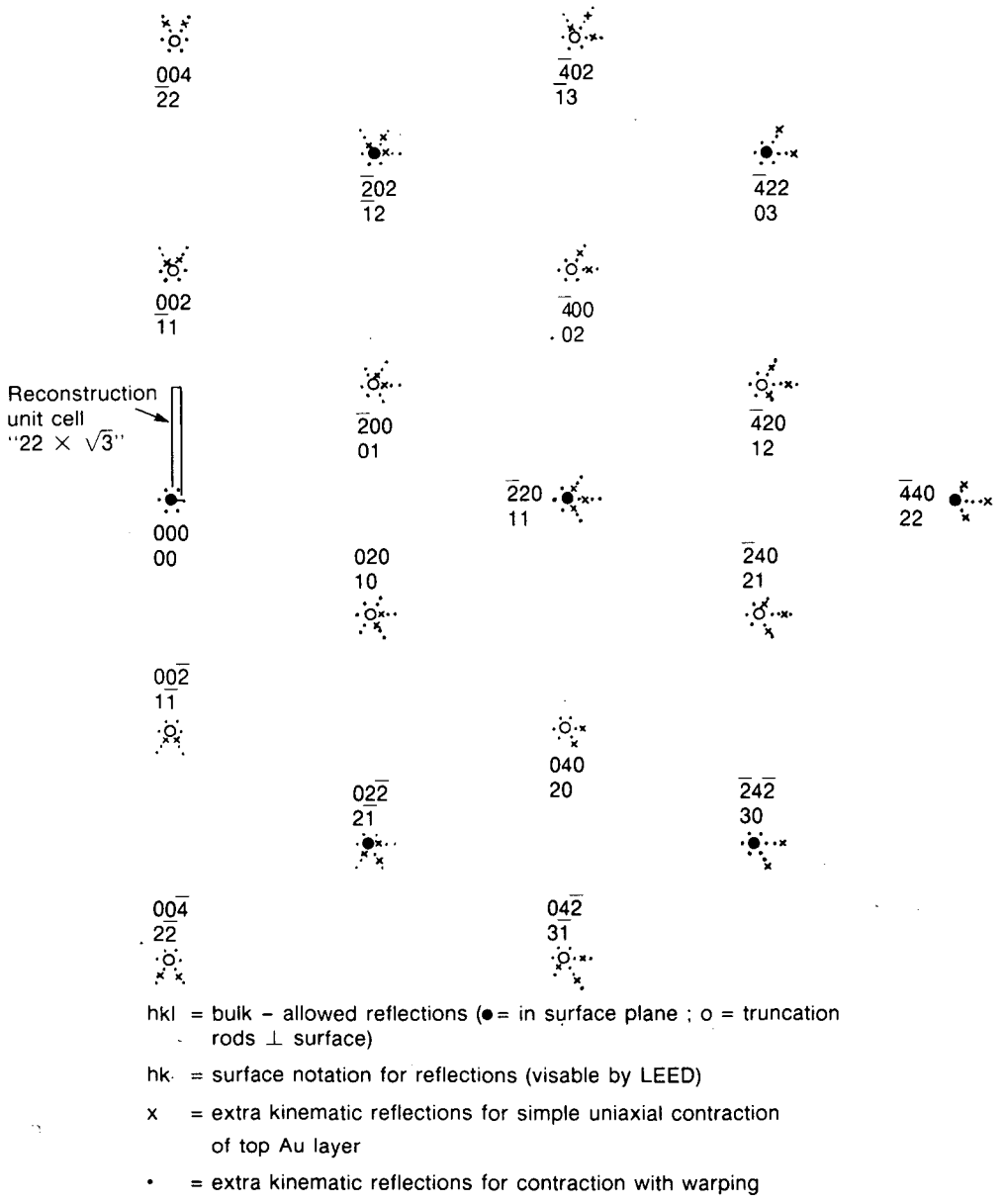

Fig. 3. Mapping of three-dimensional x-ray diffraction reciprocal space into two-dimensional LEED reciprocal space for Au(111)-($\sqrt{3}\times 22$) reconstructed surface.

<000> to <220> to <440>, in which the superlattice spots should be seen as side bands on the <220> and <440> reflections. Figure 4 shows this scan, and it is clear that the side bands were not observed. Given the difficulties with the sample handling in these preliminary experiments, it is not surprising that evidence for reconstruction was not found. It is, however, now clear where the future experimental work should be concentrated.

A structural model for the reconstructed surface has been determined. Based on earlier electron- and atom-diffraction experiments, various suggestions for this structure have been made. A calculation of expected x-ray diffraction intensities has been programmed as a function of the various structural parameters that characterize these models. It is now possible, given experimental measurements of the diffraction intensities, to determine the surface structure of Au(111) by fitting of these parameters.

Experimentally, plans for the acquisition of a rotating anode source and a four-circle diffractometer were formalized in June 1986 in collaborations among AFRD, MCSD, and CAM. This facility will allow for in-house (LBL) experiments and will permit more effective use of the limited beam time available at SSRL. The UHV system is being modified with a portable transfer vessel that will attach directly to the diffractometer.

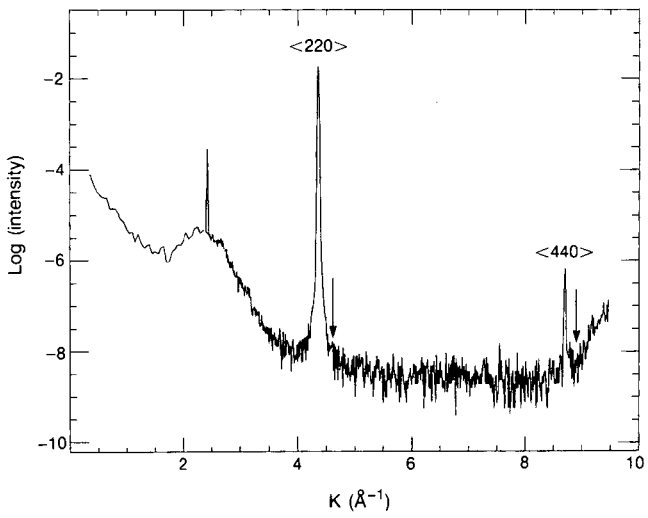

Fig. 4. In-plane scan of diffracted intensity from Au(111) near the critical angle for total reflection ($\phi = 0.35°$). Peaks indicated are diffraction from ⟨220⟩ and ⟨440⟩ bulk planes. Arrows indicate expected locations of super lattice bands for the ($\sqrt{3}\times 22$) reconstructed surface.

Study of Soft Phonon Modes and Solid-Solid Phase Transitions

Principal Investigators: Peter Y. Yu

Funding: $28,200

Project Description

Design of a facility, based on the diamond anvil cell, for performing high-pressure measurements at low temperature, and development of a technique for making four-probe electrical conductivity measurements inside the diamond anvil cell.

Accomplishments

The main difficulty in using the diamond anvil cell for high-pressure measurements is the introduction of wires into the cell. Since the wires are pressed by the diamond anvils against a steel gasket, they are easily cut off by the diamond anvil or shorted to the gasket. Both of these problems were solved by surrounding the wires with fine alumina powder. Under compression, the alumina powder formed a strong insulating layer around the wires, preventing it from being pinched by the diamond anvils. However, the use of a powder between the diamond and the gasket made it impossible to use liquid as a pressure medium since the liquid could pass through the powder when compressed. This difficulty was overcome by using a soft powder such as talc or gypsum as the pressure medium. Since all liquids would solidify at the high pressure and low temperature required for this experiment, there is no disadvantage to using the powder.

For the first time, a superconducting transition has been measured at pressures exceeding 45 GPa. The theoretical predictions of Cohen et al. concerning superconductivity in the high-pressure primitive phase of Si have been shown to be qualitatively but not quantitatively correct. The pressure dependence of the superconducting transition temperature in Si strongly suggests that transition temperatures are enhanced near solid-solid phase transitions, presumably due to soft phonon modes as suggested by the theory.

The technique developed in this project will allow various electrical measurements, not just conductivity, to be performed in diamond anvil cells as easily as optical measurements. It opens the possibility of measuring the electrical conductivity and superconducting transition temperature of hydrogen under megabars of pressure. The significance of achieving metallic hydrogen is enormous, and the results will impact fields ranging from condensed-matter physics and molecular and atomic physics to planetary physics.

The agreement between theory and experiment in Si is strongly suggestive of the importance of soft-phonon modes in enhancing superconducting transition temperatures. This mechanism has been suggested to account for the high superconducting transition temperature in crystals with the A15 structure, such as Nb_3Ge. A future experiment that can demonstrate this relationship conclusively would be to measure the phonon spectrum of Si as a function of pressure using superconducting tunnel junctions inside the diamond anvil cell. If such a relation between superconducting transition temperature and soft-phonon modes were indeed established, it will be a major step towards the search for high-temperature superconductors.

Publications

M.L. Cohen, R.J. Jeanloz, and P.Y. Yu, "High Pressure Physics," Condensed Matter Physics Seminar at the Physics Department, U.C. Berkeley, May 7, 1986.

D.J. Erskine and P.Y. Yu, "Dependence of Superconducting Transition Temperature on Pressure in Primitive Hexagonal Si," *Phys. Rev. Lett. 56*, 2270 (1986).

D.J. Erskine, P.Y. Yu, K.J. Chang, and M.L. Cohen, "Superconductivity and Phase Transitions in Compressed Si to 45 GPa," *Phys. Rev. Lett. 57*, 2741 (1986).

D.J. Erskine and P.Y. Yu, "Pressure Dependence of the Superconducting Transition Temperature of Lead and Silicon," presented at the March Meeting of the American Physical Society held at Las Vegas, NV, March 31–April 4, 1986.

D.J. Erskine, P.Y. Yu, K.J. Chang, and M.L. Cohen, "Stability of the Si Lattice: Electron-Phonon Interactions and Superconductivity in Hexagonal Si," presented at the 18th International Conference on the Physics of the Semiconductors held at Stockholm, Sweden, August 11–15, 1986.

E. Reiner and C. Radke, "Stability and Mean Field Studies of Colloidal Phase Boundaries," 60th ACS Meeting on Colloidal and Surface Science, Georgia Institute of Technology, Atlanta, June 15–16, 1986.

E. Reiner and C. Radke, "A Variational Approach to Electrostatic Free Energies of Colloids," 60th ACS Meeting on Colloidal and Surface Science, Georgia Institute of Technology, Atlanta, June 15–16, 1986.

E. Reiner and C. Radke, "Phase Behavior of Concentrated Colloids," 16th International Congress of Pure and Applied Physics, Boston, Massachusetts, August 10–16, 1986.

H.-C. Tsai, D.B. Bogy, D.K. Veirs, M. Hilton, and S. Mayer, "Structure and Properties of Sputtered Carbon Overcoats on Rigid Magnetic Media Disks," to be submitted.

Nuclear Science Division

Search for Quark-Gluon Plasma

Principal Investigator: Walter M. Geist

Funding: $123,00 (second year of funding)

Project Description

Development of a new research direction within the relativistic heavy-ion program. This project is focused on an experiment to search for enhanced production of strange baryons and antibaryons in ultrarelativistic collisions at the CERN SPS. A strong enhancement is one of the anticipated signatures of the formation of the quark-gluon plasma.

Accomplishments

NA-36, an experimental search for the quark-gluon plasma via enhanced strangeness production, is a unique and very promising approach being undertaken by a collaboration of over 60 scientists from thirteen institutions. Data collection began in November 1986 with 17 days of running with ^{16}O ions of energies at 60 and 225 GeV/nucleon. A second run will take place in September 1987.

During FY 1986, construction and installation of most major components of the experiment were completed. Key LBL contributions to this experiment—the TPC (Time Projection Chamber) and active target and beam tag—were installed in the summer of 1986. Tests with proton and $^{16}0$ beams have allowed debugging of the TPC system; preliminary calorimeter data were obtained in the November $^{16}0$ run.

Physics results from this experiment will not be available until 1987. It is clear, however, that experience gained at CERN will be of great importance in planning future experiments at higher energies, such as at the proposed Relativistic Heavy Ion Collider facility.

Large Einsteinium Activation Program (LEAP)

Principal Investigator: Darleane C. Hoffman

Funding: $92,400

Project Description

Exploratory experiments were performed using available actinide targets and "light" heavy-ion beams to produce transfermium isotopes in order to determine the best production methods and to devise the best experiments and techniques to be used when a large einsteinium target becomes available.

Accomplishments

Upgrading of the rotating wheel and data acquisition system (MG-RAGS) at the 88-Inch Cyclotron has continued. The reliability of the system has been improved, and considerable effort was spent on software development, e.g., programs for data analysis, and development of a time-correlation analysis technique for sequential alpha decay. This method was used, for example, in the identification of the isotope of element 105 with mass number 262 produced in reactions of ^{249}Bk with $^{18}0$ (Figure 1). By looking for the parent alpha energy followed closely in time by the alphas from the 4.3-s ^{258}Lr, a unique identification of $^{262}105$ can be made. A similar situation exists for the alpha decay of the unknown isotope $^{263}105$ and its 5.4-s ^{259}Lr daughter. The use of this time-correlated technique to search for sequential alpha decays permitted the measurement of the cross section for production of $^{262}105$ as 2 nb. In a search for a relatively long-lived $^{263}105$, (half-life > 10 minutes), one set of time-correlated alphas was observed that could be due to the decay of $^{263}105$ and its daughter ^{259}Lr. Obviously, additional

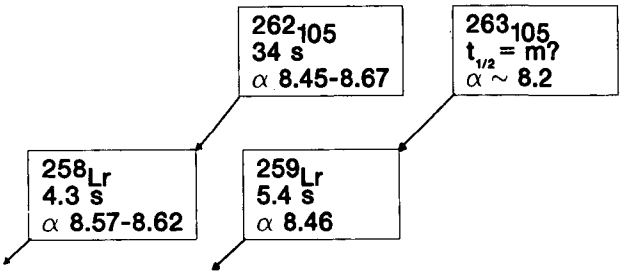

Fig. 1. The alpha decay of $^{262}105$ and $^{263}105$ leading to the decay of the short-lived Lr daughters.

experiments to confirm this result must be performed.

Enough suitable alpha-spontaneous-fission detectors have now been acquired to complete the upgrade of the fission capability, but the amplifier upgrade is still in progress. The addition to the off-line alpha-fission detector system is partially completed and has been used for alpha and fission analysis of heavy actinides produced in light heavy-ion bombardments of heavy actinide targets. This work is an important part of the continuing program to understand the reaction mechanism in order to optimize the conditions for production of actinides and transactinides. Using the detection systems at the 88-Inch Cyclotron, preliminary results for the ionic radius of lawrencium were obtained. Development of the fast automated chemistry systems for performing such studies is in progress. Collaborative experiments with LLNL on ^{254}Es + ^{18}O have shown that ^{261}Lr has a half-life of about 35 minutes and ^{262}Lr a half-life of several hours. These results confirm the predictions that spontaneous fission of the heaviest elements is stabilized by an odd neutron or odd proton and that longer-lived isotopes could be found in this region. This is very promising for the studies of chemical and nuclear properties, especially spontaneous fission of the heaviest elements.

Development work on the Small Angle Separator System (SASSY) II has continued. Effort has gone into data reduction programs, and calculations concerning the magnetic trajectories of recoil particles through the spectrometer were performed. These indicated some need for changes in the magnets, which have now been completed.

Workshops and Planning: Quark Matter '86 Conference

Principal Investigator: Lee S. Schroeder

Funding: $29,300

Project Description and Accomplishments

This project helped develop two research areas important to the Nuclear Science Division — the Bevalac Upgrade and the search for the quark-gluon plasma. The Bevalac Upgrade encompasses replacing the existing weak-focusing synchrotron at the Bevatron with a modern, strong-focusing synchrotron. Such a facility would provide the quality (emittance, duty factor) and high beam intensity needed to push beyond the pioneering heavy-ion physics program started at the Bevalac. In order to assess the physics potential and the new instrumentation required for such an effort, discussions with experimental and theoretical colleagues were carried out and presentations at two international conferences on the physics potential of the Bevalac Upgrade were presented.

In addition to its sizable program at the Bevalac to explore what has now become the domain of "intermediate-energy" heavy-ion physics (i.e., physics at 1-2 GeV/nucleon), the Nuclear Science Division has for many years been pushing for the exploration of physics to much higher energies. At these energies, anywhere from 10–100 times the Bevalac energy range, one hopes to create and examine a new phase of matter—the quark-gluon plasma. During April 13–17, 1986, the Nuclear Science Division sponsored Quark Matter '86. This was the premier meeting held on the topic since Quark Matter '84 at Helsinki in June 1984. The meeting attracted over 170 scientists from Europe, Japan, and the United States, representing 70 institutions and laboratories. The latest theoretical estimates and experimental detection schemes were examined during this brief but intense meeting. The proceedings of the conference appeared as a special edition of *Nuclear Physics A* (printed by North-Holland) in January 1987. The discussions that developed at this meeting are already being translated into results with the new high-energy heavy-ion programs just started at the Brookhaven AGS (14 GeV/nucleon) and the CERN SPS (200 GeV/nucleon).

Publications

R.M. Chasteler, R.A. Henderson, D. Lee, K.E. Gregorich, M. Nurmia, R.B. Welch, and D.C. Hoffman, "Excitation Functions for Production of Actinides from Reactions of $^{16}0$ Ions on ^{249}Cf," presented at the 192nd National ACS Meeting, Anaheim, CA, Sept. 7–12, 1986, Paper No. NUCL-8.

A. Ghiorso, "Recoil Spectrometer for Detection of Single Atoms of Heavy Elements," presented at the Conference on Methods and Applications of Radioanalytical Chemistry, Kona, Hawaii, April 5–10, 1987.

K.E. Gregorich, R. Henderson, M. Nurmia, D. Lee, R. Chasteler, H. Hall, C. Gannett, D. Bennett, and D.C. Hoffman, "Transfer of B and C Fragments from O^{18} Projectiles to Heavy Actinide Targets," presented at the 192nd National ACS Meeting, Anaheim, CA,September 7–12, 1986, Paper No. NUCL-7.

H.L. Hall, C.M. Gannett, D. Bennett, D. Lee, K.E. Gregorich, R.A. Henderson, and D.C. Hoffman, "Production Cross Sections for Heavy Actinides in the Bombardment of ^{249}Bk with ^{18}O," presented at the 192nd National ACS Meeting, Anaheim, CA, Sept. 7–12, 1986, Paper No. NUCL-10.

R.A. Henderson, R.J. Silva, K.E. Gregorich, M. Nurmia, H.L. Hall, C.M. Gannett, D. Bennett, R.M. Chasteler, Y.Y. Chu, and S. Cai, "Radiochemical Studies of Lawrencium," presented at the 192nd National ACS Meeting, Anaheim, CA, Sept. 7–12, 1986, Paper No. NUCL-11.

D.C. Hoffman, "Transuranium Isotopes," *Nucl. Instr. and Meth. A249*, 13 (1986).

D.C. Hoffman, "Transfer Reactions with Heavy Elements," presented at the Symposium on 10 Years of Uranium Beam at the UNILAC, Darmstadt, West Germany, April 2–4, 1986, (LBL-21384).

D.C. Hoffman, "Pre-LEAP Activities," presented at the 32nd Meeting of Research Materials/ Transplutonium Program Committee, Anaheim, CA, September 11–12, 1986.

D.C. Hoffman, "Atom-At-A-Time Radiochemical Separations of the Heaviest Elements," presented at the Conference on Methods and Applications of Radioanalytical Chemistry, Kona, Hawaii, April 5–10, 1987.

L.S. Schroeder, "Relativistic Heavy Ion Facilities—Worldwide," presented at the 2nd Conference on the Intersections Between Particle and Nuclear Physics, Lake Louise, Alberta, Canada, May 25–31, 1986.

L.S. Schroeder, "Probing Nuclear Matter with Dileptons," presented at the VIII International Seminar on High Energy Physics Problems, Relativistic Nuclear Physics and Quantum Chromodynamics, Dubna, USSR, June 19–24, 1986.

L.S. Schroeder and M. Gyulassy, *Proceedings of the International Conference on Ultra-Relativistic Nucleus-Nucleuc Collisions*, Pacific Grove, CA, April 13–17, 1986 (North-Holland Publishing Co., January 1987).

Physics Division

XXIII International Conference on High Energy Physics

Principal Investigator: Stewart C. Loken

Funding: $20,800

Project Description

LBL was selected as the host for the XXIII International Conference on High Energy Physics. This conference is held every two years and is hosted on a rotating basis at institutions in the United States, Europe, the Soviet Union, and Japan.

Accomplishments

The conference, attended by approximately 1600 physicists from more than 40 countries, consisted of three days of parallel sessions and three days of plenary sessions. The parallel sessions were used for reports on recent work. The plenary sessions were devoted to reviews of the parallel sessions. The proceedings of the conference, published in early 1987, consists of two volumes (~ 1500 pages) that include 15 review papers and about 300 contributed papers.

Automated Telescope Software and Hardware Development

Principal Investigator: Richard A. Muller

Funding: $191,200

Project Description

An automated telescope system was developed to systematically search for the hypothesized solar companion star (Nemesis).

Accomplishments

A search for a solar companion, based on observation of its large (3-arc-second) parallax, has been undertaken. The initial phase of this search, which employs the automated telescope system to inspect several thousand catalogued faint red stars in the northern hemisphere, will be completed within a year. A photographic system with automated plate analysis is also being developed for searching the southern hemisphere.

The possibility of catastrophic terrestrial extinctions caused by impacts were investigated. A theory of how the tidal gravitational forces of the galaxy on the Oort Cloud cause the infall of comets and how a companion star would produce comet showers has been developed. Most recently, an explanation of how small impacts can trigger geomagnetic reversals was proposed.

Advanced Semiconductor Devices for High Energy Physics

Principal Investigators: David R. Nygren and Helmuth G. Spieler

Funding: $245,700

Project Description

The SSC will require major developments in detector capabilities to exploit this new domain of energy, luminosity, and event complexity. Several workshops and a HEPAP task force on detector R&D have identified critical problems in tracking, calorimetry, triggering, data processing, electronics, radiation effects, lepton identification, and vertex detection. Long-range goals emphasize detectors that will provide nonprojective three-dimensional position information with readout speeds commensurate with the bunch structure of the SSC. An essential ingredient of such devices is the integration of detector elements and readout circuitry. Potential schemes involve combinations of both existing and emerging technology, and this work requires extensive device modeling, fabrication of test structures, and electrical measurements in order to relate device physics and performance. Requirements for devices are strongly affected by circuit and system design; hence, a substantial amount of useful information and experience can be acquired by using a standard integrated circuit (IC) process to develop devices for short-term applications in current

detectors. Thus, the work emphasized: (1) custom IC design for detector readout systems; and (2) new device structures.

Accomplishments

The design of a full custom integrated readout chip for large-scale semiconductor strip detector systems was initiated as a feasibility study for Collider Detector Facility (CDF) at Fermilab. In addition to 128 preamplifier stages, this IC contains hit detection and sparse readout circuitry, which represents a significant step beyond previous designs. Prototype chips have been received from the foundry, and initial tests confirm the feasibility of the major design objectives.

Test devices fabricated in the microelectronics laboratory on the UC Berkeley campus have provided critical information needed for the design of low-power, low-noise junction field effect transistors. These devices could provide radiation hardness in excess of 10 Mrad, essential to operation close to the interaction region of the SSC. Successful operation of these devices is crucial to future pixel arrays for vertex detection and tracking at the SSC.

Integrated Readout Systems. The proposed silicon vertex detector for CDF exemplifies the type of detector that relies on the availability of highly integrated low-noise electronics. The design of a second-generation readout chip has begun, in collaboration with the LBL CDF group, as a feasibility study for this detector. A new design is necessary for the following reasons:

- The strip length in the proposed design is substantially greater than in previous designs (Mark II, Delphi). The resulting high capacitance of 30 pF reduces the signal-to-noise ratio of the existing monolithic readouts designed at Stanford and Duisburg/Munich to impractical levels.
- The power dissipation of both existing designs is excessive.
- The large number of detector elements in the CDF design (>36,000) necessitates a sparse readout capability; i.e. in addition to the preamplifier stages and output multiplexer, the chip must include a set of level discriminators and channel-select logic.

This new device is in all respects a second-generation chip; it combines extensive analog and digital circuitry, and, furthermore, the analog circuitry must be optimized to provide enhanced performance and additional functions while significantly reducing power consumption.

The LBL chip includes 128 preamplifiers with associated discriminator circuitry. The outputs of the discriminators are fed to the readout logic, which can operate in three modes:

1. The analog outputs of all channels are read out.
2. Only those channels are read out whose associated discriminator recorded a hit.
3. All "hit channels" plus their neighbors are read out (this allows interpolation to improve position resolution). Hit addresses are also provided.

The discriminators use switched capacitor baseline restoration in order to dynamically establish a reference baseline relative to which both the signal and threshold levels are measured. This technique—unique to CMOS—allows use of the same circuit path for both the signal and introduction of the threshold level; this automatically compensates for channel-to-channel variations in amplifier gain. The circuit allows correlated double sampling for suppression of low-frequency noise or triple-correlated sampling that will also compensate for baseline shift due to detector leakage current.

The front end was designed for minimum power consumption at the required noise level and response time. Preliminary data show an equivalent noise charge of 1200 electrons at 10-pF detector capacitance and 100-ns response time. The power dissipation is about 150 mW for the complete 128-channel chip; the preamplifier stages require 0.4 mW per channel. This compares quite favorably with previous designs that require 10 to 20 times more power for the preamplifiers alone. Figure 1 shows a photograph of the 6 mm × 6 mm die, bonded to a chip carrier for test purposes.

Apart from its immediate application to CDF, this project has some general importance:

- On-chip integration of analog and digital functions to provide preselection of event readout is representative of architectures that will be extremely important in future detectors.
- This design demonstrates the benefits of tailoring circuit design to a specific application instead of simply adapting mainstream circuitry.

- This project uses design tools and a fabrication facility that are readily available to the HEP community. The design tools, e.g. SPICE and MAGIC, are public-domain software available from UC Berkeley. Chip fabrication uses a standard foundry process.
- The circuit and design techniques employed in this device are directly extendable to considerably more sophisticated devices for the next generation of detectors.

This project has found considerable interest at other laboratories, both in the U.S. and abroad. Detailed exchanges of information have taken place with the DELPHI group at Rutherford Appleton Laboratory, which is working on a less-ambitious design. A set of extended presentations at the 1986 Summer Study on the Design and Utilization of the Superconducting Super Collider in Snowmass sparked considerable interest, and several other groups in the U.S. are now seriously preparing to enter this field.

New Device Structures. The possibilities of new devices that will provide the combination of segmentation, signal-to-noise ratio, speed, low power dissipation, and radiation hardness required for the SSC are limited both by semiconductor physics and feasible fabrication techniques. Processing is currently the main limitation, and detailed studies of semiconductor device fabrication processes are necessary for several important reasons:

- Current fabrication processes for strip detectors still have poor control over surface effects. This leads to poor yields and environmental sensitivity. Surface problems are exacerbated in pixel devices due to the larger periphery of the structures. Mainstream semiconductor fabrication does not use high-resistivity silicon, and industry will not solve this problem.
- Radiation-hard processes have been developed for aerospace and military applications, but they must be adapted to specific devices. Again, mainstream R&D in this area does not use high-resistivity substrates.
- Shallow-junction FET structures that should provide low-noise, low-power devices with a radiation hardness in excess of 10 Mrad (this is an order of magnitude higher than can be obtained with MOSFET's) have been proposed. High-resistivity substrates would allow junction isolation with the low capacitance necessary for the high-speed low-power circuitry needed for the SSC.
- Integration of detectors and readout electronics will be essential for large-scale pixel devices. This should be accomplished either by monolithic integration or by hybrid structures that bond separate detector and readout chips. Both schemes entail technological uncertainties that require detailed investigation in order to arrive at viable production devices.

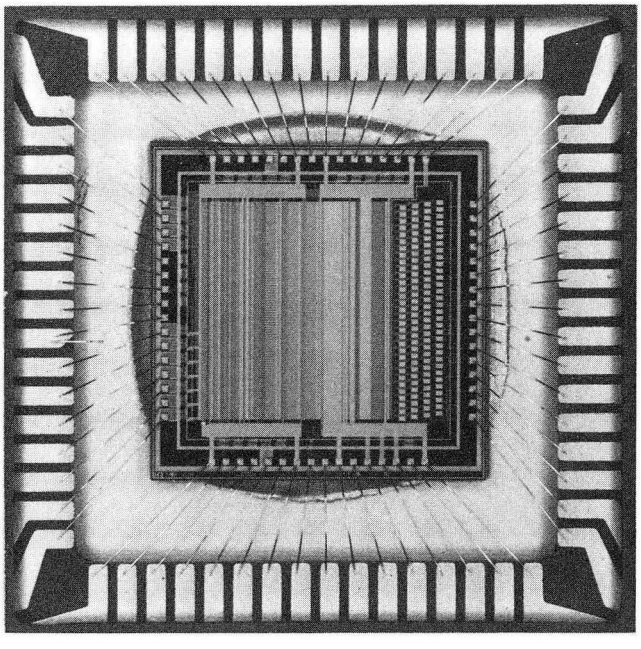

Fig. 1. An intergrated readout system for silicon strip detectors. This chip combines analog and digital circuitry to provide 128 channels of low-noise low-power preamplifiers with circuitry for data preselection and data output logic.

Several "generations" of detector test structures have been fabricated using the IC facility on campus. A typical test device consists of a central diode (detector) surrounded by a combined MOS transistor and guard-ring structure. This allows separation of bulk and surface currents and also provides information on the density of interface states and the surface mobility. Again, a multitude of measurements must be performed and sifted to obtain bits of information, and it is premature to state results. These devices show good bulk-carrier lifetime, suitable for both high-quality detectors and transistors. However, they still show excessive surface currents. The current process may be adequate for junction FETs, and new masks are being prepared to include these

devices on the next wafers. This is especially interesting since these devices offer both low power dissipation and high resistance to radiation damage.

Computer simulation is an important tool in this work; extensive use has been made of SUPREM III, a process-simulation code developed at Stanford University. One- and two-dimensional device simulators (SEDAN and PISCESII, also from Stanford) have also been installed that can take a SUPREM output file describing a realistic device structure and determine its electrical characteristic. A code developed by Spieler is used to determine hot-electron effects on noise in field-effect transistors. This has provided valuable insight into new FET designs that could combine low noise, low power, and high radiation hardness. A synopsis of these results was presented at the SSC Workshop in Snowmass.

Although much work remains, the first results are encouraging, showing that good quality detectors can be made with the same equipment used for ICs on less-critical substrates. However, the limitations of this equipment have also been experienced, especially for low-temperature deposition of oxide and nitride films, where cleanliness seems inadequate. The new Center for Integrated Systems at Stanford University should offer improvements, and tests will be arranged as soon as the appropriate equipment is operational.

Conclusion. LBL has embarked on a new program that breaks new ground for high-energy physics. The first phase has been completed of a custom IC design program that goes substantially beyond previous designs and tests a path for use of this technology by the high-energy-physics community. A substantial amount of preparatory work necessary to apply advanced semiconductor technology to high-energy physics in the areas of new devices—especially for pixel arrays—and radiation hard structures has been completed. Extensive discussions with interested experimentalists from this country and abroad have taken place, and all have expressed enthusiasm for this program, which could lead to a unique semiconductor R&D capability for high-energy physics.

Development of Gas-Scintillation Drift Chamber

Principal Investigator: Bernard Sadoulet

Funding: $66,200

Project Description

The gas-scintillation drift chamber involves a novel technique for detecting electrons extracted by charged particles produced in a gas by x or gamma rays. It is based on gas scintillation, which occurs when electrons drift in a relatively high electric field. This method potentially has the advantages of ionization chambers in terms of linearity and absence of space-charge effect but brings in a large signal-to-noise improvement. For high-pressure operation, high spatial or pulse-height accuracy applications and high-rate environments, it is expected to surpass significantly the conventional detection technique by electron avalanche. This is especially true if one uses a read-out technique using wave shifter fibers. It provides an elegant way of extracting the light and is well adapted to the use of high pressure. The two-dimensional read-out can be implemented by allowing half of the light to go through the first layer and be collected by another layer at 90 degrees. The time of occurrence of the photon interaction can be obtained from the primary scintillation of the gas. This will provide a time zero for the fifth measurement and allow three-dimensional imaging.

This technique can be quite interesting for particle physics, especially when low space charge, high spatial accuracy, or high energy resolution is needed. However, the main motivation was hard x-ray astrophysics. High-pressure gas-scintillation drift chambers could literally revolutionize the field by providing:

- Large area and good stopping power;
- High energy resolution;
- High spatial resolution to provide the best angular resolution and three-dimensional imaging capability in order to image naturally

complex events (photoelectric interaction with escape photon, Compton scatter, and pair production); and

- Good background rejection through the use of an escape photon that signifies a K-shell photo-interaction.

The goals this year were mainly to build a prototype to test these ideas and to begin investigating the potential technical problems listed below.

- *Gas Purity.* Impurities will quench both the primary scintillation and the secondary scintillation in the high field gap. This required building a clean chamber with only ceramics and metals.
- *Relatively High Voltages.* The present prototype, for instance, requires 60 kV, though with very small currents. However, proper engineering and production of high voltage directly in the chamber allows the potential problems to be minimized.
- *High Pressure.* The detector has been designed to operate at the maximum practical pressure with xenon at 40 atmospheres.

Accomplishments

The chamber has been built. All of the parts, including the HV feedthroughs and seals, are ceramic or metal, and the chamber has passed a safety check for operation at 40 atmospheres. An all-metal gas system has also been assembled, and the fiber holder is ready. As a first step, the prototype chamber has been assembled with a quartz window behind which the light is collected by sixteen half-inch-square phototubes (Figure 2). The chamber has been operated at 5 atmospheres and detected 60-keV x rays from an americium source. Though the electronics are still rather unsophisticated, spectra have been observed (Figure 3), and the light yield in the scintillation gap has been estimated. The results roughly agree with previous literature on gas-scintillation chambers. Furthermore, the electrical breakdown characteristics also agree with expectations. Finally, the light fibers to be used in the second phase of the project do not contaminate the gas severely.

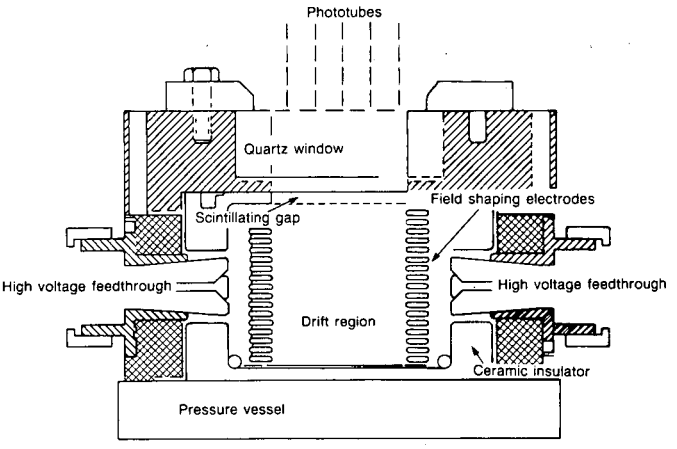

Fig. 2. Engineering drawing of GSDC prototype.

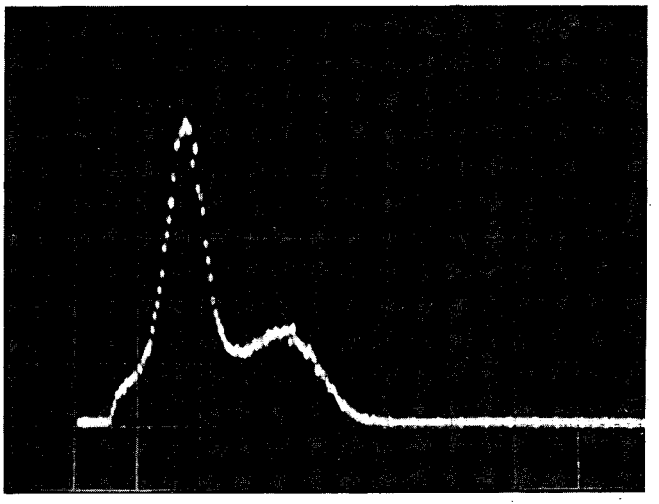

Fig. 3. ^{241}Am spectrum taken with prototype GSDC (with gas exposed to wave shifting light fibers).

Antiproton 30th Anniversary Celebration

Principal Investigator: George H. Trilling

Funding: $16,700

Project Description

Organization of Antiproton 30th Anniversary Celebration.

Accomplishments

"Antiprotons: Past, Present, and Future" was the theme of a two-day conference commemorating the thirtieth anniversary of the discovery of the antiproton. The meeting, held at Booth Hall on the UC Berkeley campus November 15–16, 1986, was attended by almost 200 participants from all over the world. Distinguished speakers and session chairmen included five Nobel laureates—Luis Alvarez, Owen Chamberlain, Carlo Rubbia, Emilio Segrè, and Simon Van der Meer—and many others who were involved in the historic discovery at the Bevatron thirty years ago. Presentations covered the historic origins of the discovery, the impact of the discovery and current research to which it led, and future directions for the field of high-energy physics.

Publications

L. Bosisio, "Silicon Detectors—Status and Plans for Experiments at SPS, Tevatron, SLC, and LEP," presented at the Third Pisa Meeting on Advanced Detectors, Castiglione della Pescaia, Italy, June 2–7, 1986.

S. Kleinfelder, "VLSI Design Techniques," 1986 Summer Study on the Design and Utilization of the Superconducting Super Collider, Snowmass, CO, June 23–July 11, 1986.

S.C. Loken, Editor, *Proceedings of the XXII International Conference on High Energy Physics*, July 16–23, 1986, Berkeley, CA, Vols. I and II, World Scientific Publishing Co. Singapore (1987).

D.E. Morris, "Diffuse Galactic Matter Does Not Cause Comet 'Death Showers'," LBL-20650 (1986).

D.E. Morris and R.A. Muller, "Tidal Gravitational Forces: The Infall of New Comets and Comet Showers," *Icaris 65*, 1 (1986).

R.A. Muller and D.E. Morris, "Geomagnetic Reversals from Impacts on the Earth," *Geophysical Research Letters 13*, 1177 (1986).

B. Sadoulet, R.P. Lin, and S. Weiss, "Gas Scintillation Drift Chambers with Wave Shifter Read-Out for Hard X-Ray Astronomy," to be published in *IEEE Transactions of Nuclear Science.*

B. Sadoulet, R.P. Lin, T. Prince, K. Hurley, and W. Pietsch, "High Energy All Sky Imager (HEASI) Explorer," NASA proposal, University of California preprint (1986).

H. Spieler, "Preamplifier Design in the Monolithic Age," 1986 Summer Study on the Design and Utilization of the Superconducting Super Collider, Snowmass, CO, June 23–July 11, 1986.

H. Spieler, "Pixel Devices with Ultra-Fast Readout," 1986 Summer Study on the Design and Utilization of the Superconducting Super Collider, Snowmass, CO, June 23–July 11, 1986.

H. Spieler, "Semiconductor Sensors," Workshop on Applications and Prospects for Semiconductors Detectors, Rutherford Appleton Laboratory, U.K., May 17–18, 1986.

LAWRENCE BERKELEY LABORATORY
OFFICE FOR PLANNING AND DEVELOPMENT
UNIVERSITY OF CALIFORNIA
BERKELEY, CALIFORNIA 94720